

AD-A056 326

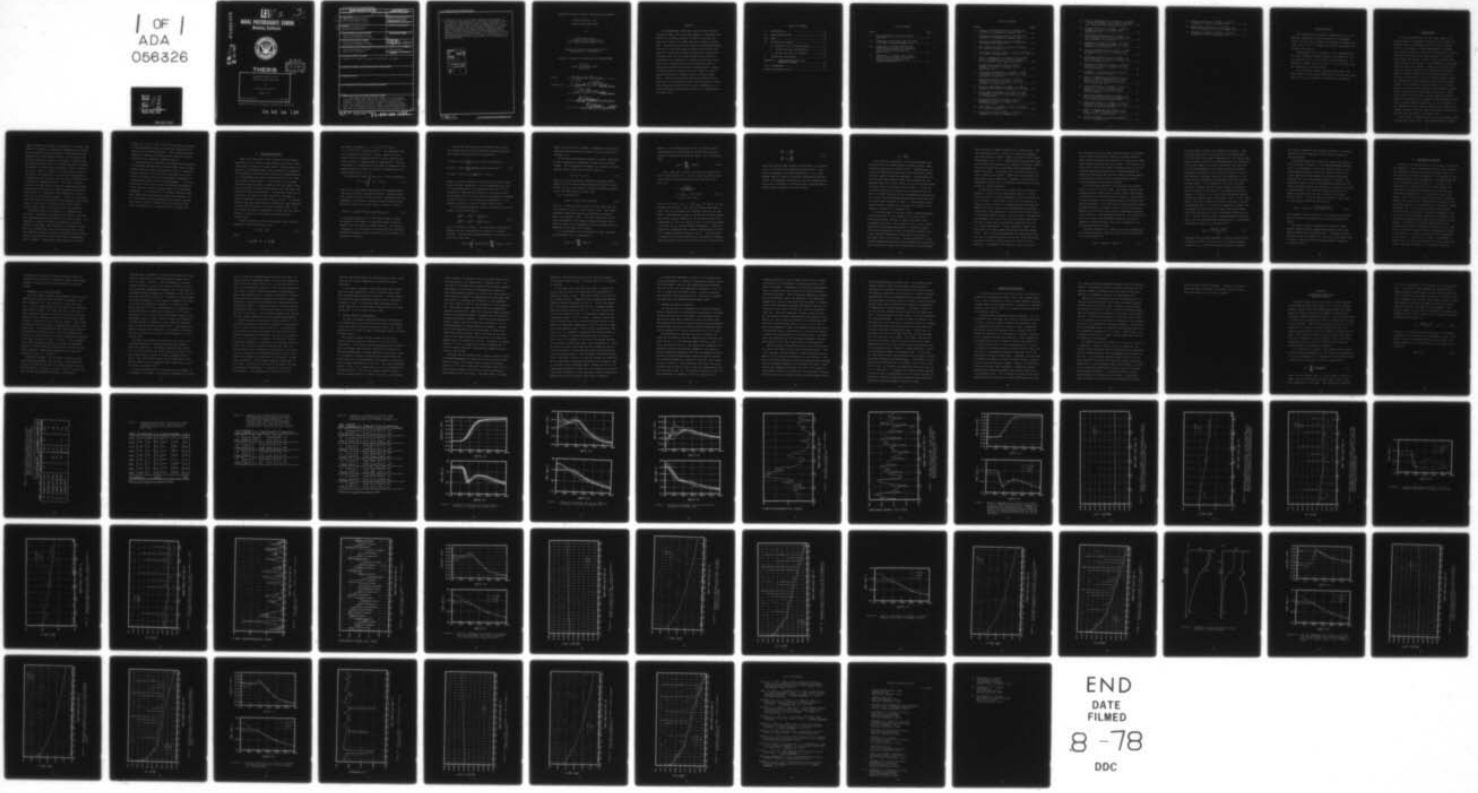
NAVAL POSTGRADUATE SCHOOL MONTEREY CALIF  
SALINITY EFFECTS IN AN OCEAN MIXED-LAYER MODEL.(U)  
MAR 78 R A PAULUS

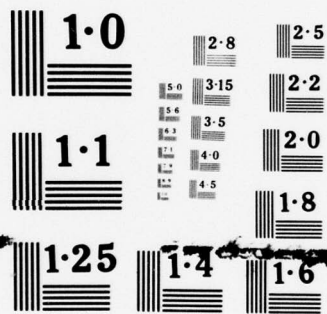
F/G 8/10

UNCLASSIFIED

NL

1 OF 1  
ADA  
056326





NATIONAL BUREAU OF STANDARDS  
MICROCOPY RESOLUTION TEST CHART

AD A 056326

LEVEL II

2

NAVAL POSTGRADUATE SCHOOL  
Monterey, California

SC

ID No.   
DC FILE COPY



DDC  
RECEIVED  
JUL 18 1978  
RECEIVED

# THESIS

SALINITY EFFECTS IN AN  
OCEANIC MIXED-LAYER MODEL

by

Richard Alan Paulus

March 1978

Thesis Advisor: R. L. Elsberry

Approved for public release; distribution unlimited.

78 07 10 133

REPORT DOCUMENTATION PAGE		READ INSTRUCTIONS BEFORE COMPLETING FORM	
1. REPORT NUMBER	2. GOVT ACCESSION NO.	3. RECIPIENT'S CATALOG NUMBER	
4. TITLE (and Subtitle) Salinity Effects in an Ocean Mixed-Layer Model		5. TYPE OF REPORT & PERIOD COVERED Master's Thesis, March 1978	
7. AUTHOR(s) Richard Alan/Paulus		6. PERFORMING ORG. REPORT NUMBER	
9. PERFORMING ORGANIZATION NAME AND ADDRESS Naval Postgraduate School Monterey, California 93940		8. CONTRACT OR GRANT NUMBER(s)	
11. CONTROLLING OFFICE NAME AND ADDRESS Naval Postgraduate School Monterey, California 93940		10. PROGRAM ELEMENT, PROJECT, TASK AREA & WORK UNIT NUMBERS	
14. MONITORING AGENCY NAME & ADDRESS (if different from Controlling Office) Naval Postgraduate School Monterey, California		12. REPORT DATE March 1978	13. NUMBER OF PAGES 77
		15. SECURITY CLASS. (of this report) Unclassified	
		16a. DECLASSIFICATION/DOWNGRADING SCHEDULE	
16. DISTRIBUTION STATEMENT (of this Report) Approved for public release; distribution unlimited.			
17. DISTRIBUTION STATEMENT (of the abstract entered in Block 20, if different from Report)			
18. SUPPLEMENTARY NOTES			
19. KEY WORDS (Continue on reverse side if necessary and identify by block number)			
20. ABSTRACT (Continue on reverse side if necessary and identify by block number) A one-dimensional mixed-layer model of ocean thermal structure (Camp, 1976) was first modified to determine the effects of a salinity profile on density structure and secondly to observe the added effects of surface salinity flux. The model was tested in August and November-December 1974 with (1) hydrocast data at Ocean Stations HOTEL and PAPA and (2) salinity profiles statistically derived from <span style="float: right;">cont</span>			

251 454

act

historical data for six ocean stations and adjusted to correspond to an observed BT. Inclusion of salinity structure did not significantly affect mixed-layer depth or temperature predictions during the summer period. During the winter period, salinity structure tended to inhibit deepening yielding a slightly warmer, shallower mixed layer. Surface salinity flux altered significantly the thickness of the isothermal layer, with decreases in thickness during precipitation ( $E-P < 0$ ) and a tendency for increased thickness during some periods of net downward heat flux when  $E-P > 0$ .

ACCESSION for		
NTIS	White Section	<input checked="" type="checkbox"/>
GDS	Dist Section	<input type="checkbox"/>
UNANNOUNCED		<input type="checkbox"/>
JUSTIFICATION		
BY		
DISTRIBUTION/AVAILABILITY CODES		
SPEC. AVAIL. NO./OF SPECIAL		
A		

Approved for public release; distribution unlimited.

Salinity Effects in an  
Oceanic Mixed-Layer Model

by

Richard Alan Paulus  
Lieutenant, United States Navy  
B.S., Iowa State University, 1970

Submitted in partial fulfillment of the  
requirements for the degree of

MASTER OF SCIENCE IN METEOROLOGY AND OCEANOGRAPHY

from the  
NAVAL POSTGRADUATE SCHOOL  
March 1978

Author

Richard A. Paulus

Approved by:

Russell L. Elsberry

Thesis Advisor

R. W. Garwood by RRE

Second Reader

G. J. Haltiner

Chairman, Department of Meteorology

G. J. Haltiner (acting)

Dean of Science and Engineering

## ABSTRACT

A one-dimensional mixed-layer model of ocean thermal structure (Camp, 1976) was first modified to determine the effects of a salinity profile on density structure and secondly to observe the added effects of surface salinity flux. The model was tested in August and November-December 1974 with (1) hydrocast data at Ocean Stations HOTEL and PAPA and (2) salinity profiles statistically derived from historical data for six ocean stations and adjusted to correspond to an observed BT. Inclusion of salinity structure did not significantly affect mixed-layer depth or temperature predictions during the summer period. During the winter period, salinity structure tended to inhibit deepening yielding a slightly warmer, shallower mixed layer. Surface salinity flux altered significantly the thickness of the isothermal layer, with decreases in thickness during precipitation ( $E-P < 0$ ) and a tendency for increased thickness during some periods of net downward heat flux when  $E-P > 0$ .

TABLE OF CONTENTS

I.	INTRODUCTION - - - - -	11
II.	MODEL MODIFICATIONS - - - - -	14
III.	DATA - - - - -	20
IV.	DISCUSSION OF RESULTS - - - - -	25
	A. HYDROCAST VS. BT INITIALIZATION - - - - -	26
	B. TYPICAL PROFILE INITIALIZATION - - - - -	29
	C. SOURCES AND SINKS OF SALINITY - - - - -	32
V.	SUMMARY AND CONCLUSIONS - - - - -	35
APPENDIX A.	HYDROCLIMATOLOGICAL DATA	
	RETRIEVAL PROGRAM - - - - -	38
	LIST OF REFERENCES - - - - -	75
	INITIAL DISTRIBUTION LIST - - - - -	76

LIST OF TABLES

Table	Page
I. Data availability at ocean station locations - - - - -	40
II. Comparison of STP casts with BT traces at OS PAPA, November-December 1974 - - - - -	41
III. Comparison of forecast SST and MLD among different model initialization runs and with observations for August 1974 - - - - -	42
IV. Comparison of forecast SST and MLD among different model initialization runs and with observations for November-December 1974 - - - - -	43

## LIST OF FIGURES

Figure	Page
1. Overplot of hydrocast data for OS Papa for the period 21 November-31 December 1974 - - - -	44
2. Overplot of hydrocast data for OS HOTEL for the period 21 November-31 December 1974 - - - -	45
3. Overplot of hydrocast data for OS HOTEL for the period 8-28 August 1974 - - - - - - - - - -	46
4. Wind stress at OS PAPA - 18 GMT 23 November to 18 GMT 06 December 1974 - - - - - - - - - -	47
5. Total heat flux at OS PAPA - 18 GMT 23 November to 18 GMT 06 December 1974 - - - - - - - - - -	48
6. Depth vs temperature and salinity at OS PAPA 18 GMT 23 November and 18 GMT 06 December 1974, hydrocast data, neglecting (E-P) - - - -	49
7. Surface salinity at OS PAPA - 18 GMT 23 November to 18 GMT 06 December 1974, neglecting (E-P) - - - - - - - - - - - - - - - -	50
8. Mixed-layer temperature at OS PAPA - 18 GMT 23 November to 18 GMT 06 December 1974 from hydrocast initialization - - - - - - - - - - - -	51
9. Mixed-layer depth at OS PAPA - 18 GMT 23 November to 18 GMT 06 December 1974 from hydrocast initialization - - - - - - - - - - - -	52
10. Depth vs temperature at OS PAPA - 18 GMT 23 November and 18 GMT 06 December 1974, BT data -	53
11. Mixed-layer temperature at OS PAPA - 18 GMT 23 November to 18 GMT 06 December 1974 from BT initialization - - - - - - - - - - - - - - - -	54
12. Mixed-layer depth at OS PAPA - 18 GMT 23 November to 18 GMT 06 December from BT initialization - - - - - - - - - - - - - - - -	55
13. Wind stress at OS HOTEL - 14 GMT 28 November to 14 GMT 29 December 1974 - - - - - - - - - -	56
14. Total heat flux at OS HOTEL - 14 GMT 28 November to 14 GMT 29 December 1974 - - - - - - - -	57

15.	Depth vs temperature and salinity at OS HOTEL - 14 GMT 28 November and 14 GMT 29 December 1974, hydrocast data, neglecting (E-P) - - - -	58
16.	Surface salinity at OS HOTEL - 14 GMT 28 November to 14 GMT 29 December 1974, neglecting (E-P) - - - - - - - - - - - - - -	59
17.	Mixed-layer temperature at OS HOTEL - 14 GMT 28 November to 14 GMT 29 December 1974 from hydrocast initialization - - - - - - - -	60
18.	Mixed-layer depth at OS HOTEL - 14 GMT 28 November to 14 GMT 29 December 1974 from hydrocast initialization - - - - - - - - - -	61
19.	Depth vs temperature at OS HOTEL - 14 GMT 28 November and 14 GMT 29 December 1974, BT data - - - - - - - - - - - - - - - -	62
20.	Mixed-layer temperature at OS HOTEL - 14 GMT 28 November to 14 GMT 29 December 1974 from BT initialization - - - - - - - - - - -	63
21.	Mixed-layer depth at OS HOTEL - 14 GMT 28 November to 14 GMT 29 December 1974 from BT initialization - - - - - - - - - - - - -	64
22.	Schematic of a derived salinity profile assuming a typical buoyancy - - - - - - - -	65
23.	Depth vs temperature and salinity at OS HOTEL - 14 GMT 28 November and 14 GMT 29 December 1974, BT and typical salinity data, neglecting (E-P) - - - - - - - - - -	66
24.	Surface salinity at OS HOTEL - 14 GMT 28 November to 14 GMT 29 December 1974, neglecting (E-P) and using a typical salinity profile - - - - - - - - - - - - -	67
25.	Mixed-layer temperature at OS HOTEL - 14 GMT 28 November to 14 GMT 29 December 1974 from typical profile initialization - - - - -	68
26.	Mixed-layer depth at OS HOTEL - 14 GMT 28 November to 14 GMT 29 December 1974 from typical profile initialization - - - - - - - -	69
27.	Depth vs temperature and salinity at OS HOTEL - 14 GMT 28 November and 14 GMT 29 December 1974, hydrocast data - - - - - - -	70
28.	(E-P) at OS HOTEL - 14 GMT 28 November to 14 GMT 29 December 1974 - - - - - - - - -	71

- 29. Surface salinity at OS HOTEL - 14 GMT 28  
November to 14 GMT 29 December 1974 - - - - - 72
- 30. Mixed-layer temperature at OS HOTEL - 14  
GMT 28 November to 14 GMT 29 December 1974 - - - 73
- 31. Mixed-layer depth at OS HOTEL - 14 GMT 28  
November to 14 GMT 29 December 1974 - - - - - 74

## ACKNOWLEDGEMENTS

The author wishes to express appreciation to Dr. R. L. Elsberry, Department of Meteorology, Naval Postgraduate School, for his time, interest, and guidance throughout this study, and to Dr. R. W. Garwood for helpful discussions and review of this thesis.

Appreciation is also expressed to the Commanding Officer, Fleet Numerical Weather Central, for permission to use the facilities and to the staff for their assistance. In particular, thanks is due to LCDR. H. D. Sturr for his time and assistance in obtaining data.

The author additionally expresses gratitude to his wife, Janet, for her understanding while this work was being done and for her assistance in preparing the manuscript.

## I. INTRODUCTION

It has been established that the upper layer of the ocean responds to atmospheric forcing on the synoptic and diurnal time scales [Elsberry and Camp (1978), Garwood (1977)]. The success of those models which incorporate only mechanical mixing, convective overturning, and vertical diffusion in predicting the time evolution of the mixed layer (Camp and Elsberry, 1978) has shown the short term ocean boundary layer response to be predominately one-dimensional in many ocean regimes. Although the general model [see Camp (1976)] contains both temperature and salinity effects, Camp and Elsberry (1978) considered density as a function of temperature only, and assumed buoyancy flux to the atmosphere to be attributable to the heat flux alone. Johnson (1977) followed with an evaluation of the model's ability to forecast ocean thermal structure based on atmospheric forcing derived from synoptic-scale data. Again, due to lack of salinity data, Johnson neglected salinity effects and therefore had to adjust initial temperature profiles to remove positive gradients. It is the purpose of this research to study salinity effects on the upper ocean thermal structure using the Camp (1976) model by making comparisons with the results of Johnson (1977).

Miller (1976) included salinity in the mixed layer model of Kraus and Turner (1967). Using BOMEX Period III upper

ocean soundings, he showed, for periods up to 10 days, the effects of salinity on mixed-layer temperatures and depths and the effects of precipitation on surface salinity and temperature in the tropical Atlantic. He concluded that the most significant effect of inclusion of salinity was the reduced cooling rate of the mixed layer due to reduced entrainment of water from the pycnocline into the base of the layer. This is a result of a larger density jump at the base of the layer when a salinity jump corresponds to a temperature jump than would be the case if density were a function of temperature alone. This type of density structure can also lead to a positive temperature gradient (temperature increasing with depth) immediately below the mixed layer (i.e. the mixed-layer temperature is cooler than that of the underlying water). Miller also concluded that the effects of precipitation were greatest under conditions of light winds and heavy rainfall during which a shallow stable layer is produced at the ocean surface.

Considering Miller's findings, it is apparent that salinity is important in determining the density structure when applying a mixed-layer model to the entire ocean. Furthermore, although the relative importance of salinity effects on the short term evolution of the density profile may not be significant, one would anticipate that a long term imbalance between evaporation and precipitation contributes to the buoyancy flux and could lead to significant density changes. Additionally, sound speed in the ocean

varies by  $1.2$  to  $1.3 \text{ ms}^{-1} (\text{‰})^{-1}$  and salinity variations in the near-surface layers can thus have significant effects on the sound-speed profile. These effects would be greatest in regions of varying surface salinity flux and advection (e.g., doldrums, subpolar regions).

The importance of salinity in the model and the paucity of concurrent temperature and salinity data, even at ocean weather stations, raise the question of how to incorporate salinity effects into the initial conditions and to then verify the results when the only available information is a temperature profile from a bathythermograph. It was the objective of this study to test the salinity contribution to the density structure observed based on two different approaches: (1) utilization of available hydrocasts when both temperature and salinity profiles are available, and (2) utilization of bathythermographs and typical temperature/salinity profiles derived from the historical data files and adjusted to be compatible with an observed BT.

## II. MODEL MODIFICATIONS

Camp (1976) and Miller (1976) presented the governing equations for the vertical redistribution of heat and turbulent kinetic energy in the upper ocean. These equations, as applied to a well-mixed layer, were simplified by appropriate assumptions and closure was achieved by parameterization of the dissipation and shear production terms of the turbulent kinetic energy budget. At the surface, the boundary conditions were specified in terms of the wind stress, insolation, sensible and latent heat fluxes, back radiation, and evaporation minus precipitation. The boundary conditions at the base of the layer are then computed by the model in terms of the fluxes of momentum, heat, and salt. In developing the numerical scheme from the expressions, Camp neglected salinity effects because of a lack of salinity data. For this study, the model was modified to account for the contributions of salinity to the density structure and the buoyancy flux.

A linear equation of state was assumed, which, when expressed in terms of buoyancy,  $B$ , is

$$B = \alpha gT - \beta gS \quad (2-1)$$

where

$$\alpha = -\frac{1}{\rho_0} \frac{\partial \rho}{\partial T} \quad \text{and} \quad \beta = \frac{1}{\rho_0} \frac{\partial \rho}{\partial S}$$

are taken as constant;  $\alpha = 2.5 \times 10^{-4} (\text{°C})^{-1}$  and  $\beta = 7.5 \times 10^{-4} (\text{°/oo})^{-1}$  after Camp (1976). The assumption that  $\beta$  is constant is quite good. However, density is not a linear function of temperature and  $\alpha$  can be taken as constant only over a limited range of temperatures. The density profile is represented in the model as temperature and salinity pairs to a depth of  $-N\Delta Z$  by  $N$  isothermal and isohaline slabs of  $\Delta Z (= 2.5 \text{ m})$ .

The potential energy (PE) per unit is then expressed as

$$PE = -\rho_0 g \int_{-D}^0 (\alpha T - \beta S) Z dZ \quad (2-2)$$

where  $D$  is a fixed depth greater than the maximum penetration of the vertical turbulent processes. Assuming advective processes and the variation due to compressibility are negligible, the change in potential energy resulting from mixing the layer from a depth  $-N\Delta Z$  to a depth  $-(N+1)\Delta Z$  is

$$\Delta PE(N) = \frac{1}{2} \rho_0 g N (\Delta Z)^2 [\alpha (T_N - T_{N+1}) - \beta (S_N - S_{N+1})] \quad (2-3)$$

If  $\alpha (T_N - T_{N+1}) - \beta (S_N - S_{N+1}) > 0$ , the water column is stable and  $\Delta PE_m(N)$  is the amount of turbulent kinetic energy required to mix the layer to a depth  $-(N+1)\Delta Z$ . If  $\alpha (T_N - T_{N+1}) - \beta (S_N - S_{N+1}) < 0$ , the column is unstable and will overturn, generating turbulent kinetic energy by free convection (represented as  $\Delta PE_c(N)$ ).

In each one hour time step the model first accounts for surface fluxes, and the resulting temperature profile and surface (N=1) salinity are determined by

$$\begin{aligned}
 T_1(t+\Delta t) &= T_1(t) + \frac{\Delta t}{\rho_o c_p} [-Q_T(0, t^*) + Q_S(0, t^*) - Q_S(-\Delta Z, t^*)] \\
 T_N(t+\Delta t) &= T_N(t) + \frac{\Delta t}{\rho_o c_p} [Q_S(-N\Delta Z, t^*) - Q_S(-(N+1)\Delta Z, t^*)] \quad (2-4) \\
 S_1(t+\Delta t) &= S_1(t) + S_1(t) \frac{\Delta t}{\Delta Z} [E(t^*) - P(t^*)]
 \end{aligned}$$

where  $Q_S$  is solar radiation,  $Q_T$  is the sum of latent, sensible, and back radiation,  $E$  is the evaporation rate, and  $P$  is the precipitation rate during the interval  $t^* = \Delta t$ . Insolation is distributed vertically in the water column by absorbing 50% in the first meter and absorbing the remaining 50% as  $\exp(-\gamma Z)$ . The extinction coefficient,  $\gamma$ , was assumed constant at  $0.002 \text{ cm}^{-1}$  after Johnson (1977).

If the resulting buoyancy profile is unstable, the water column is mixed according to

$$\begin{aligned}
 T_{N+1}^{(i+1)} &= (NT_1^{(i)} + T_{N+1}^{(i)}) / (N+1) \\
 S_{N+1}^{(i+1)} &= (NS_1^{(i)} + S_{N+1}^{(i)}) / (N+1)
 \end{aligned} \quad (2-5)$$

until the profile is stable. The temperature and salinity profiles are then isothermal and isohaline to a depth  $-(N+1)\Delta Z$ . The potential energy generated by this free convection is found from

$$\Delta PE_c = -\rho_o g \int_{-D}^0 (\alpha \delta T - \beta \delta S) Z dZ \approx \sum_{N=1}^{NN-1} \Delta PE_c(N) \quad (2-6)$$

where  $\delta T$  and  $\delta S$  are the changes in temperature and salinity resulting from mixing and the depth of free convection is  $(NN)(\Delta Z) \leq D$ .

If the resulting buoyancy profile is stable, additional kinetic energy must be expended to further mix the water column. The total amount of energy,  $E_T$ , available for mixing the first  $N$  levels with the  $N+1$  level is

$$E_T = E_m + E_c - E_p \quad (2-7)$$

where  $E_m$  is the mechanically generated turbulent kinetic energy,  $E_c$  is the convectively generated turbulent kinetic energy, and  $E_p$  is the amount of energy previously expended to mix the water column to depth  $-N\Delta Z$ .

$E_m$  is calculated by

$$E_m(N) = [\rho_o w_*^3 \exp(-N\Delta Z/H)] \Delta t \quad (2-8)$$

with  $w_*$  = average friction velocity in the ocean over the time interval  $\Delta t$  and  $H$  = scale depth of 50 m. This depth-dependent formulation follows the approach of Elsberry, Fraim, and Trapnell (1976). Setting a scale depth of  $H=\infty$  would correspond to the original Kraus and Turner (1967) model in which the net generation minus dissipation was independent of the depth of the layer.

$E_c$  is considered to be the fraction of  $\Delta PE_c$  available for entrainment and is calculated as

$$E_c(N) = -R \sum_{N=1}^{NN-1} \Delta PE_c(N) \quad (2-9)$$

where  $R = 0.15$  following Camp (1976) and Johnson (1977), and represents the percentage of convectively generated energy not dissipated by viscous forces.  $E_p$  is calculated from

$$E_p(N) = \sum_{i=N}^{N-1} \Delta PE_m(i) \quad (2-10)$$

If  $E_T > \Delta PE_m$  for  $N$  levels, then there is energy available to mix to level  $N+1$ . If  $E_T < \Delta PE_m$ , the level is partially mixed following Thompson (1976) and Camp (1976).

Thus, let

$$a = \frac{NE_T(N)}{(N+1)\Delta PE_m(N)}$$

$$\bar{Q} = [aQ_{N+1} - (N-a)Q_N]/N \quad (2-11)$$

$$\bar{Q}' = aQ_N + (1-a)Q_{N+1}$$

and set  $Q_i = \bar{Q}$  for  $i=1,2,\dots,N$  and  $Q_{N+1} = \bar{Q}'$  where  $Q$  is temperature and salinity. Note that the mixing algorithms require that the isothermal and isohaline layers be the same depth. The mixed-layer depth is determined from the temperature profile only by defining it as the depth at which the temperature is  $0.2^\circ\text{C}$  less than  $T_1$ , where  $T_1$  has been assumed to be equal to  $T_0$ , the sea-surface temperature. Light wind conditions, strong heating, or heavy precipitation could result in some difference between  $T_1$  and  $T_0$ . The pycnocline is assumed to be weakly diffusive and the change of temperature and salinity below the well-mixed layer is specified by

$$\frac{\partial T}{\partial t} = A_v \frac{\partial^2 T}{\partial Z^2}$$

$$\frac{\partial S}{\partial t} = A_v \frac{\partial^2 S}{\partial Z^2}$$

(2-12)

where the vertical eddy diffusion coefficient,  $A_v$ , is taken to be  $0.5 \text{ cm}^2\text{-sec}^{-1}$  after Haney and Davis (1976). This value is consistent with many observations. It is much greater than the values of molecular conductivity and diffusion. The processes involved are not well understood but may be due to breaking of internal waves, double diffusion, and/or lateral advection on a small scale.

### III. DATA

This study used atmospheric and bathythermograph data extracted from the Fleet Numerical Weather Central (FNWC) historical data file by Johnson (1977). Additionally, the 12-hour accumulated precipitation field produced by FNWC's primitive equation model was extracted. Oceanographic station data for Ocean Station HOTEL were obtained from the National Ocean Data Center (NODC) and for Ocean Station PAPA from the Institute of Ocean Sciences (1975). The data at OS HOTEL consisted of 18 Nansen cast observations and the data at OS PAPA consisted of three hydrographic observations and 11 STP (salinity-temperature-pressure) observations for the time frames indicated in Table I. Additionally, daily surface salinity samples were available at OS PAPA for the period 06 December to 31 December 1974.

To take advantage of the more numerous bathythermograph (BT) observations, it was proposed to use some type of historical salinity profile in conjunction with a BT to initialize the model. One possibility was to use a profile generated from climatological means at different depths. This proved unfeasible in that the profiles contained very little detailed information on the salinity structure in the upper levels of the ocean. Another possibility, using standard temperature-salinity relationships for a water mass, was rejected since these relationships fail in the boundary

layer because of changes caused by the surface fluxes. The third possibility was to utilize the Hydroclimatological Data Base Retrieval (HYDAT) system installed at FNWC (Ocean Data Systems, Inc., 1977). HYDAT retrieves hydroclimatological data from the historical and synoptic data bases. FNWC's historical files contain expendable bathythermograph and Nansen cast data. The synoptic file contains the most recent 72 hours of BT reports. HYDAT then statistically analyzes these data as described in Appendix A and selects a temperature profile that is considered typical for the time period ( $\geq$  1 month) specified.

If the typical profile is a Nansen cast, the salinity profile is output with the temperature profile. If the typical profile is a bathythermograph, then no salinity profile is given. In this case, it may still be possible to obtain a salinity profile by searching manually through the HYDAT output for a Nansen cast sounding whose sea-surface temperature, deep temperature, and heat content come closest to fitting the median values. For this study, the parameters were weighted such that the fit of sea-surface temperature and heat content were considered more important than the fit of deep temperature. In some locations, Nansen casts were sparse and their parameters deviated from the median values. Thus, a minimum requirement for considering a Nansen cast as a typical profile was that the three parameters must fall within the range between the first and third quartiles. Proceeding in this manner, salinity profiles

were obtained for all six ocean weather stations in December and for three ocean weather stations in August (Table I). These salinity profiles were assumed to be typical for these ocean station locations and time of year. More ideally, one would like to have a data bank of hydrocast data and an extracting system which would take a bathythermograph and search the historical data for the closest fitting temperature profile and then use the corresponding historical salinity profile as the typical profile.

Once the typical profiles were obtained, the question arose as to how to utilize them. The initial observed temperature profile likely has structural details that should be reflected in the initial salinity profile. These details include the depth of the well-mixed layer and positive temperature gradients. Thus the typical salinity profile should be mixed as deep as or deeper than the BT and the salinity gradient should be such that positive temperature gradients do not lead to an unstable density profile. The typical profiles for a month were therefore treated in two ways to generate a salinity profile that would correspond to any specified BT for that month.

The first method was to combine the typical temperature and salinity profiles,  $T_T(Z)$  and  $S_T(Z)$  into a typical buoyancy profile  $B_T(Z)$ , by

$$B_T(Z) = \alpha g T_T(Z) - \beta g S_T(Z) \quad (3-1)$$

and the buoyancy profile was checked for stability. Then the mixed-layer depth, the depth where the temperature is  $0.2^{\circ}\text{C}$  less than the surface temperature, of the typical temperature profile and of the bathythermograph were determined. If the layer depth of the  $T_T(Z)$  profile was less than that of the bathythermograph, the buoyancy profile was mixed according to equations (2-5) to the layer depth of the BT. This mixing is necessary because of the assumption in the model that the isothermal and isohaline layers are mixed to the same depth. If the mixing were not done, the model would use a certain amount of input energy in mixing the salinity profile to the level of the temperature profile, whereas, in reality, it is likely that the actual salinity profile was already mixed to the deeper level. If the layer depth of the  $T_T(Z)$  profile was greater than that of the BT, no mixing was done. If a positive temperature gradient was encountered in the BT before the layer depth was reached, the BT was considered to have a mixed-layer depth equal to zero. Finally, with any given bathythermograph observation,  $T_O(Z)$ , and the assumed buoyancy profile  $B_T(Z)$ , a corresponding salinity profile,  $S_O$ , was found from

$$S_O(Z) = \frac{\alpha g T_O(Z) - B_T(Z)}{\beta g} . \quad (3-2)$$

Therefore this procedure generates a salinity profile from an observed profile consistent with the typical buoyancy profile, (3-1). Since this buoyancy profile is based on

the typical temperature and salinity profiles, it is representative of the conditions at that location during the specified month.

The second method was to take the typical salinity profile and match it directly to the bathythermograph observation. The advantage of the typical salinity profile over a climatological profile is that the typical profile is an actual observation and therefore has detailed structural features that the climatological profile is lacking. The mixed-layer depth of the BT was determined as above and the typical salinity profile was required to be mixed to the same or greater depth. The resulting profiles gave rise to a buoyancy profile which was then required to be stable:  $B(Z-\Delta Z) \geq B(Z)$ . If the profile was unstable at any level,  $Z$ , the salinity profile was adjusted by

$$S_T(Z) = S_T(Z-\Delta Z) + \frac{\alpha[T_O(Z)-T_O(Z-\Delta Z)]}{\beta} \quad (3-3)$$

which assures neutral stability. A new  $B(Z)$  was calculated and the procedure continued until the entire profile was stable.

The salinity profile resulting from either of these methods permits positive temperature gradients that would appear unstable when considered alone. Including salinity therefore allows the model to be used over a much wider range of oceanic conditions without biasing potential energy as in Johnson (1977).

#### IV. DISCUSSION OF RESULTS

Initially, the salinity flux at the surface of the ocean was neglected. This is potentially accurate only if there is a balance of evaporation and precipitation (E-P) over the time period of model integration. The validity of this assumption as well as the assumption of one-dimensionality can be checked by examining Figs. 1-3. In Fig. 1, the variability of surface salinity at OS PAPA between the first STP cast (1724 GMT 23 November 1974) and the last (1730 GMT 06 December 1974) is quite small and one can safely neglect the advection and surface flux of salinity. However, the variations of temperature and salinity in the pycnocline appear to be characteristic of advective effects associated with tidal period and internal wave motion. Also notice that the positive temperature gradients in the layer 80-150 m are excellent examples of the need for corresponding salinity profiles when vertical mixing is being modeled. Variations at OS HOTEL between 1430 GMT 28 November and 1442 GMT 29 December 1974 (Fig. 2) are on the order of one-half part per thousand and generally confined to the upper 50 m. Notice that there is more variability in the pycnocline here than at OS PAPA. At OS HOTEL in August (Fig. 3), salinity variations are quite extreme even within individual soundings. The variations cannot be

accounted for by realistic surface salinity fluxes and therefore are likely due to advective effects and/or small changes in ship position and the proximity to the Gulf Stream.

#### A. HYDROCAST VS. BT INITIALIZATION

The first model run shown using hydrocast data is at OS PAPA during the period from 1800 GMT 23 November to 1800 GMT 06 December 1974. Wind stress and total heat flux, Figs. 4 and 5, respectively, for this period were extracted from the FNWC fields. The total heat flux is the sum of solar radiation, sensible and latent heat fluxes, and back radiation and is generally positive for this period, indicating an upward heat flux at the sea surface. Under these conditions, one would expect a deepening and cooling of the mixed layer. The initialization and verification profiles from STP data are shown in Fig. 6 and the predicted time evolution of surface salinity, surface temperature and mixed-layer depth are shown in Figs. 7, 8, and 9. The corresponding initial temperature profile (with positive gradients removed to ensure stability) derived from a BT and the predicted changes in mixed-layer temperature and depth are depicted in Figs. 10, 11, and 12.

Comparison of Figs. 8 and 11 shows a similar cooling trend and good agreement with the data. Notice that the initial SST from the STP cast was slightly warmer than the SST from the BT. Similarly, in Figs. 9 and 12, one can see that the STP initialization predicts a consistently

shallower MLD as compared to the BT initialization but each forecast agrees well if verified against similar type of data (see Figs. 6 and 10). This discrepancy in observed thermal structure is seen to be fairly consistent in that the sea-surface temperature averaged  $0.26^{\circ}\text{C}$  warmer and the mixed-layer depth averaged 11.4 m shallower in the STP cast data than the BT data (Table II). Taking this into account, the model performance is very similar throughout the period as the STP initialization resulted in a cooling of the mixed layer by  $0.8^{\circ}\text{C}$  and a deepening of 9.8 m whereas the BT initialization resulted in a cooling of  $0.78^{\circ}\text{C}$  and a deepening of 7.1 m. Note that the slab depth (depth of the isothermal layer) in Figs. 9 and 12 retreats and deepens in a similar manner in response to weak stress and downward heat flux as described by Johnson (1977). This would be an expected feature since salinity, in the absence of sources and sinks, would have no effect on the shoaling of the isothermal layer.

The major contribution of salinity in this case is the stabilizing effect on the positive temperature gradient below the thermocline. The salinity gradient that allows this to occur increases the density jump at the base of the mixed-layer depth and tends to inhibit deepening of the layer. This case further points out the importance of the initial profile in the subsequent model predictions, as was also shown by Johnson (1977).

The next case considers a 31-day period (28 November to 29 December) at OS HOTEL. The synoptic variability of stress

(Fig. 13) and the corresponding upward heat flux (Fig. 14) again indicate a deepening regime. The initial temperature profile from the Nansen cast in Fig. 15 and from the BT in Fig. 19 are essentially identical. The initial salinity profile (Fig. 15) shows a relative maximum at approximately 100 m, which should act as a barrier to deepening. However, below this level, salinity decreases with depth and would contribute to vertical overturning if not stabilized by the temperature profile. A gradual increase of surface salinity is predicted (Fig. 16) as more saline water is entrained at the base of the layer. This variation appears to be smaller than the natural variability in the salinity measurements.

Almost identical cooling rates of the surface of  $3.7^{\circ}\text{C}$  during the period were forecast by hydrocast initialization (Fig. 17) and BT initialization (Fig. 20). Qualitatively this follows the trend indicated by the observations, but forecasts sea-surface temperatures that are on the order of  $1.5$  to  $2.0^{\circ}\text{C}$  too cold. Likewise, a very similar trend in mixed-layer deepening is forecast by the hydrocast initialization (Fig. 18) and by the BT initialization (Fig. 21). Both forecasts tend to indicate too deep a MLD in the first 14 days as compared to observations but then tend to correspond to the data in the later half of the period. As mentioned previously, the slab depth responds identically in both cases. At the end of the period, the Nansen cast initialization is approximately 7 m shallower than the BT initialization. This difference is due solely to the

salinity structure because the same forcing is used in each case and the initial temperature profiles were nearly identical.

It may seem inconsistent that both mixed layers would have the same temperatures, since the deeper layer would have entrained more cold water from below. However, given the relatively weak temperature gradient and a difference in depth of only 7 m, the extra water entrained in the deeper layer has an insignificant cooling effect on a water column that is on the order of 100 m deep.

#### B. TYPICAL PROFILE INITIALIZATION

The lack of adequate temperature-salinity observations over large parts of the ocean was motivation for attempting to use the salinity profiles derived in Section III. Both procedures were tested in order to determine which, if either, was more useful.

The typical buoyancy profile method for deriving a typical salinity profile, Equations (3-1) and (3-2) was tested first. This method, while providing initial profiles that were stable, gave salinity profiles that were not in general representative of those observed in the ocean. That is, unrealistic salinity variations were created below the mixed layer due to the constraint that buoyancy be conserved. This is shown schematically in Fig. 22. The typical buoyancy profile in Fig. 22a is mixed from  $Z_1$  to  $Z_2$  to correspond with the MLD of the BT. The salinity profile derived from the typical buoyancy profile is shown in Fig. 22b. In the mixed

layer, buoyancy is constant, thus the derived salinity will vary according to the temperature by Equation (3-2). At the base of the mixed layer, mixing of the buoyancy profile has created an artificially strong gradient between the level where mixing stopped,  $Z_2$ , and the next layer below,  $Z_3$ . Thus salinity increases to compensate for the buoyancy jump. Below level  $Z_3$ , buoyancy has returned to a weak gradient but, this level is still in the thermocline of the observed BT. Thus salinity again decreases until the temperature gradient becomes weak. Below this, salinity again increases because the buoyancy gradient is greater than  $\alpha g$  times the observed temperature gradient. Thus, the second approach of using a typical salinity profile and adjusting it to the bathythermograph was judged superior in general. However, notice this approach has the disadvantage of producing a larger than normal salinity jump at the base of the mixed layer if the typical salinity profile has to be mixed to a greater depth to correspond to the BT. Therefore, at deeper depths, ( $> 100$  m), it might still be more appropriate to use the buoyancy approach, although this suggestion was not tested in this study.

The model was initialized with a typical salinity profile and bathythermograph at OS PAPA and run for the same 13-day period as above. The results were cooling of the mixed layer by  $0.75$  °C and a deepening of the mixed layer by  $5.17$  m which agree relatively well with the results obtained by initialization with a BT alone. One might expect a typical

profile to work relatively well at this location because the overplots shown in Fig. 1 indicate very little variation of salinity.

By the same token, one would not expect a typical profile to work as well at OS HOTEL given the variations of salinity in Figs. 2 and 3. This was tested for the same 31-day period as above. Temperature and corresponding derived salinity profiles are shown in Fig. 23. Notice that above 100 m the typical salinity profile has a stronger gradient than the actual profile in Fig. 15. Both the initial (Fig. 23) and the predicted (Fig. 24) mixed-layer salinities are consistently about 1 ‰ too fresh. However, this difference in salinity has only a relatively small effect on the predicted mixed-layer temperature in Fig. 25, which is similar to the trend in Figs. 17 and 20 with a mixed-layer cooling of 3.6 °C. Likewise the predicted mixed-layer depth in Fig. 26 displays a similar deepening trend as in Fig. 18 and is only 5 m different by the end of the period compared to the model run using the Nansen cast initialization. Thus the model has made a good forecast even though the typical salinity profile is rather different than the observed profile in the upper levels. The noticeable difference between Fig. 26 and Figs. 18 and 21 is that the mixing, as indicated by the slab depth is strongly inhibited by the salinity jump at the base of the isothermal depth. Because of the 0.2 °C temperature difference between the slab depths and the mixed-layer depth definitions, this indicates a weaker temperature gradient below the well-mixed layer than is observed.

Of particular importance in Fig. 23 is the model predicted development of a positive temperature gradient below the mixed layer. That is, the model mixed-layer temperature is  $13.78^{\circ}\text{C}$  and the temperature increases to  $13.91^{\circ}\text{C}$  at 7.5 m below the isothermal layer. A positive gradient was observed in the verification BT. This type of thermal structure was also demonstrated by Miller (1976).

### C. SOURCES AND SINKS OF SALINITY

In this section, the assumption of a long term balance between evaporation and precipitation was eased by including surface salinity flux in the model. The evaporation rate was derived from FNWC's Evaporative Heat Flux (EHF) field. The precipitation rate was obtained from 12-hour accumulated precipitation calculated by FNWC's primitive equation model and was assumed to be evenly distributed over the 12 hours.

Incorporating the salinity flux at the surface, the model was initialized with the temperature and salinity profiles in Fig. 15. The resulting model profiles, after 31 days, are shown in Fig. 27. The significant changes in the predicted salinity profile when compared to the salinity profile predicted neglecting (E-P) are the agreement of predicted and observed mixed-layer salinities and the absence of a relative maximum at the base of the mixed layer (refer to Figs. 15 and 27). The evaporation rate minus the precipitation rate is shown in Fig. 28 and the corresponding surface salinity in Fig. 29. The surface salinities in Fig. 29 show variations in response to (E-P) as opposed to the

surface salinities in Fig. 16 which show only an increase with time due to entrainment of more saline water at the base of the layer. Comparison of sea-surface temperatures [Fig. 17 without and Fig. 30 with (E-P)] shows indistinguishable forecasts. Thus sea-surface temperature changes due to inclusion of (E-P) are apparently not significant enough over a layer of this depth for the model to resolve. Finally, the slab depth responds differently under the influence of (E-P) (Fig. 31) than when (E-P) was neglected (Fig. 18). The most significant changes caused by (E-P) are the enhanced retreats (decreases in slab depth) during days 3, 10, and 18 when precipitation was significant, and inhibited retreats during days 8, 13, 17, 22, 25, and 26 when (E-P) apparently offset net downward surface heat flux. Of particular note is precipitation on day 18 which caused a retreat that corresponded to the observations. The subsequent slow deepening of the slab depth represents the gradual mixing of the stable layer formed by precipitation.

Typical profile initialization runs, both with and without (E-P), were made at other ocean station locations. Due to the sparsity of observations, no firm conclusions can be made as to the absolute verification of the forecasts. However, a relative comparison can be made among results obtained from the different methods of initializing the model. These results are summarized in Tables III and IV. The length of the forecast period was determined by the continuous forcing function data and the longest period possible between initial

and verifying thermal structure data. The different model results shown in Table III for August indicate little variability in predicted SST or MLD due to salinity effects. This might be expected, in that August is a month of strong downward heat flux and temperature effects would dominate. Thus one might be cautious about including a typical salinity profile under these conditions since there is a possibility of degrading the model performance. Included in Table IV are the results obtained during a period of net upward heat flux. One would expect salinity effects to be more important in a deepening regime. The data in Table IV indicate, for the most part, that inclusion of salinity results in a warmer and shallower mixed layer than would be the case with density as a function of temperature alone. Notice that, at OS INDIA (57N 20W) and OS MIKE (66N 02E), the MLD exceeded 300 m (the bottom of the model). This might indicate that either the "typical" salinity profile used was not really representative of the area or that horizontal advection cannot be neglected here. However, in high latitudes in winter the temperature gradient is extremely weak. In this case, the slab depth would be more indicative of the depth to which the mixing processes were penetrating. At OS INDIA, the predicted slab depths are 212.5 m (TYPPRO), 200.0 m (E-P), and 272.0 m (BT). At OS MIKE, the respective values are 281.2 m, 277.5 m, and 240.0 m. Although at OS MIKE the model appears to have run well on temperature only, the initial BT was corrected for a positive temperature gradient which would have biased the potential energy of the water column.

## V. SUMMARY AND CONCLUSIONS

It was the purpose of this study to test the effects of salinity in a mixed-layer model of the ocean thermal structure. This is desirable in that the ocean thermal structure in many areas can be explained only if salinity is considered. However, this salinity data is not always available even at ocean weather stations.

The problem was approached using two methods: (1) initialization with hydrocast data, and (2) initialization with a BT and a salinity profile derived from historical data and adjusted to correspond to the BT. First, evaporation and precipitation were assumed to be in balance over the period of integration and the effects of salinity structure on the thermal structure were observed. Then, evaporation and precipitation were included to observe the effects of a surface salinity flux on the thermal structure. The incorporation of observed salinity profiles into the model did not result in significant changes in forecasts of SST and MLD during the August period tests. Similarly, for the same conditions, inclusion of adjusted typical salinity profiles did not cause any distinct changes. However, the effects of salinity structure were noticeable in deepening regimes. Qualitatively, model performance was slightly improved by using hydrocast data. Use of adjusted typical salinity profiles and BTs also resulted in slight improvement even when

the typical profile was somewhat different than the observed profile. The general effects of salinity structure were to produce a warmer, shallower mixed layer than results when density is considered a function of temperature only.

Addition of the salinity flux due to imbalances of evaporation and precipitation did not show pronounced effects on SST or MLD in the short term. However, a long term upward buoyancy flux,  $E > P$ , tends to offset the slower entrainment rate caused by the inclusion of salinity in the density profile. The short term effects of  $(E - P)$  were most evident in the response of the slab depth as compared to the response when only the surface heat flux was considered. The retreat of the isothermal layer is enhanced during precipitation and the subsequent deepening rate is slowed. Additionally, the tendency of this layer to shoal under downward heat flux may be inhibited by evaporation.

The addition of salinity effects to the model is certainly desirable. However, salinity data are sparse and the typical salinity profiles must be applied with an understanding of the meteorological and oceanographical conditions of the area. Thus one would consider salinity data to be far more important in mid and high latitudes during a deepening regime than in low latitudes during strong heating. One must also consider the variations of salinity and the processes causing these variations. In subpolar regions, salinity varies markedly with freezing and thawing. In monsoonal areas, reversal of the wind and thus wind-induced currents,

makes advective effects important. Further, an attempt to apply the model ocean-wide would require salinity data in many areas where it is not now available.

APPENDIX A  
HYDROCLIMATOLOGICAL DATA  
RETRIEVAL PROGRAM

The Hydroclimatological Data Retrieval (HYDAT) program was designed by Ocean Data Systems, Inc. (1977) to access, process, display, and store hydroclimatological data bases. Among the outputs available from HYDAT is an option that produces a typical temperature profile. This typical profile is obtained by specifying the month (or months) and the location of interest. The location specified is taken to be the midpoint of a circular or square search area, with the original search distance from the midpoint determined by the user. If at least six reports are not found in this area, the area is expanded by fixed increments until six or more reports are found or until the maximum search distance, either default or specified, is reached.

If the search is successful, each report found is separated into three parameters: (1) the sea-surface temperature, (2) the deep temperature, a temperature at an arbitrary depth (~200 m), and (3) the heat content as computed from

$$HC = \sum_{i=1}^N \frac{[\bar{T} - (-5)] \cdot \Delta Z}{D} \quad (A-1)$$

where D is the deepest level, N is the number of layers to depth, D, ΔZ is the thickness of each layer, and  $\bar{T}$  is the mean temperature in the layer. Any sounding not extending

to D is not considered in the selection of the typical profile. The values of each parameter are then screened to remove isolated extreme values and the frequency distribution is checked for the number of modes ( $\leq 3$ ) present. All three parameters must have the same number of modes. HYDAT then computes and prints the median and first and third quartile values for each mode of each parameter. The typical profile in each mode is determined by comparing the parameter values of each profile with the median values and determining a deviation,  $D_i$ ,

$$D_i = \frac{W_i |P_i - M_i|}{M_i}, \quad i=1,2,3 \quad (A-2)$$

where  $W_i$  is a weighting factor assigned to the individual parameter,  $P_i$  is the value of the parameter, and  $M_i$  is the median value of the parameter within any one mode. The typical profile is then the report with the lowest sum of deviations:

$$\text{Sum} = \sum_i D_i \quad (A-3)$$

TABLE I. Data availability at ocean station locations. Numbers under TYPICAL PROFILE indicate the total number of profiles (both BT and hydrocast) upon which the typical profile is based.

OWS	LAT	LONG	08 - 28 August 1974			21 November - 31 December 1974		
			BT	HYDROCAST	TYPICAL PROFILE	BT	HYDROCAST	TYPICAL PROFILE
H	38°N	71°W	53	9	-	70	9	297
I	57°N	26°W	33	-	-	5	-	6
M	66°N	02°E	33	-	196	14	-	34
N	30°N	140°W	18	-	90	14	-	23
P	50°N	145°W	195	-	115	104	14	51
T	29°N	135°E	-	-	-	4	-	25

TABLE II. Comparison of STP casts with BTs at OS PAPA, November-December 1974. Observations are within one hour and ten nautical miles of each other.

DATE	SST(STP)	SST(BT)	$\Delta T$	MLD(STP)	MLD(BT)	$\Delta D$
23 Nov	8.11 °C	8.0 °C	0.11 °C	65.3* m	76.2 m	-10.9 m
24 Nov	7.90	7.6	0.3	70.9*	73.8	-2.9
26 Nov	7.87	7.6	0.27	72.1	88.7	-16.6
29 Nov	7.91	7.6	0.31	71.0	83.4	-12.4
01 Dec	7.84	7.6	0.24	65.1	81.3	-16.2
02 Dec	7.93	7.7	0.23	71.3	71.0	0.3
03 Dec	7.67	7.4	0.27	75.4	88.3*	-12.9
04 Dec	7.81	7.5	0.31	65.4	85.9	-20.5
06 Dec	7.68	7.4	0.28	76.6	86.8*	-10.2
Mean differences			0.26 °C			-11.4 m

\*Indicates positive gradient encountered above MLD.

TABLE III. Comparison of forecast SST and MLD among different model initialization runs and with observations for August 1974. HC is hydrocast data, TYPPRO is BT and typical salinity data, (E-P) indicates inclusion of surface salinity flux, and BT is temperature data. Verifying data are from BTs.

OWS PERIOD	PREDICTED PARAMETER	HC	TYPPRO	(E-P)	BT	VERIFICATION
H 12 days	SST(°C)	24.23	-	24.23	24.20	27.2
	MLD(m)	32	-	33	35	24
M 15 days	SST(°C)	-	11.44	11.42	11.27	11.4
	MLD(m)	-	28	29	32	38
N 19 days	SST(°C)	-	22.60	22.51	22.70	24.4
	MLD(m)	-	12	13	12	24
P 19 days	SST(°C)	-	13.20	13.17	13.20	12.9
	MLD(m)	-	19	19	19	29

TABLE IV. Comparison of forecast SST and MLD among different model initialization runs and with observations for November-December 1974.

OWS PERIODS	PREDICTED PARAMETER	HC	TYPRO	(E-P)	BT	VERIFICATION
H 31 days	SST (°C)	13.72	13.78	13.70	13.73	14.5
	MLD (m)	112	107*	115	119	115*
P 13 days	SST (°C)	7.31	7.25	7.32	7.22	7.4
	MLD (m)	75	81	74	83	87*
H 39 days	SST (°C)	-	14.28	14.33	14.24	14.6
	MLD (m)	-	128*	127	141	137*
I 13 days	SST (°C)	-	8.81	8.82	8.9	9.8
	MLD (m)	-	7300	7300	7300	201
M 17 days	SST (°C)	-	6.89	6.89	6.9	7.7
	MLD (m)	-	7300.	7300	247	181*
N 21 days	SST (°C)	-	20.51	20.47	20.54	19.9
	MLD (m)	-	85	88	83	54
P 35 days	SST (°C)	-	6.53	6.55	6.46	6.7
	MLD (m)	-	103	101	108	104
T 18 days	SST (°C)	-	21.59	21.57	21.56	22.2
	MLD (m)	-	93	95	96	97

\* Indicates positive gradient encountered above MLD

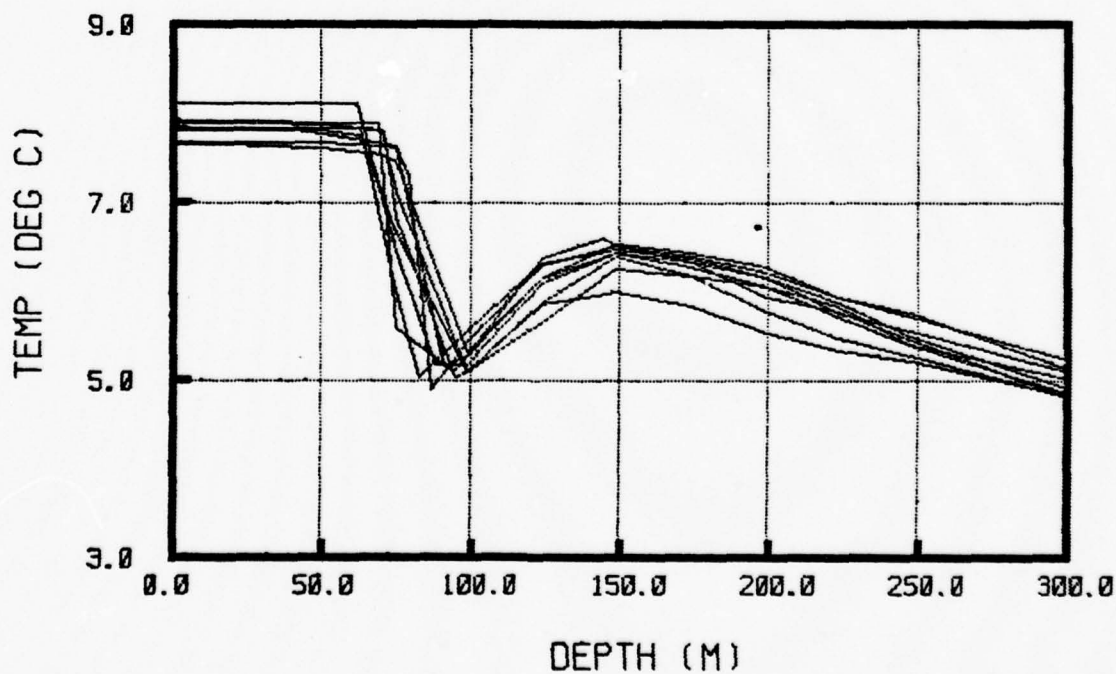
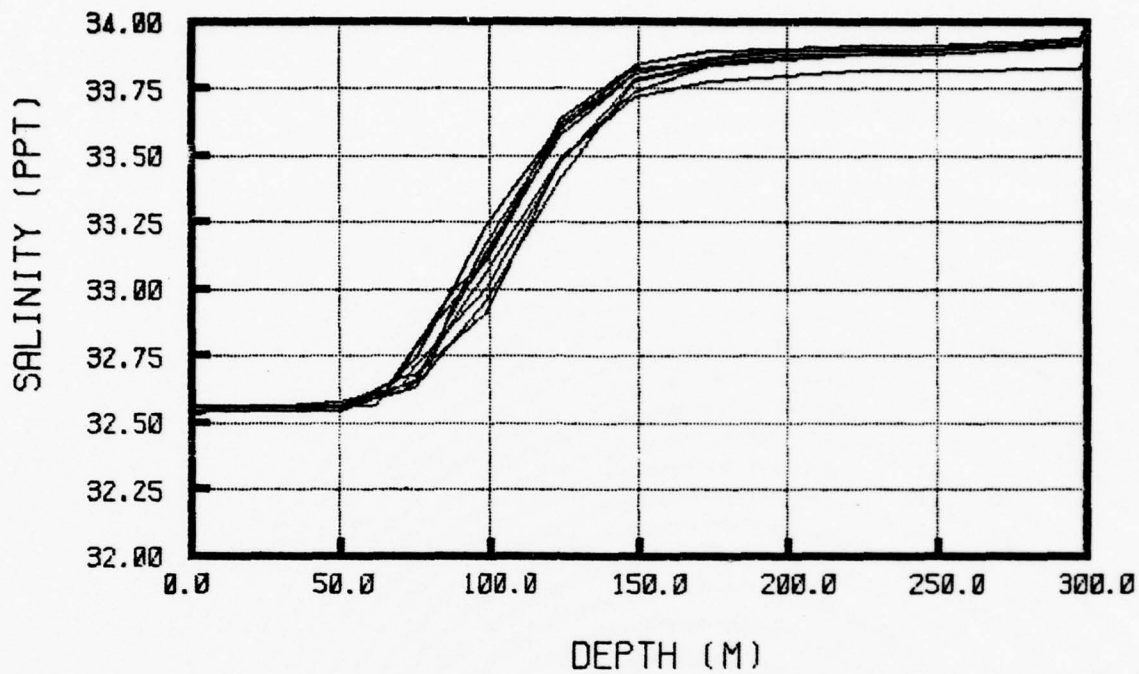


Figure 1. Overplot of hydrocast data for OS PAPA for the period 21 November-31 December 1974.

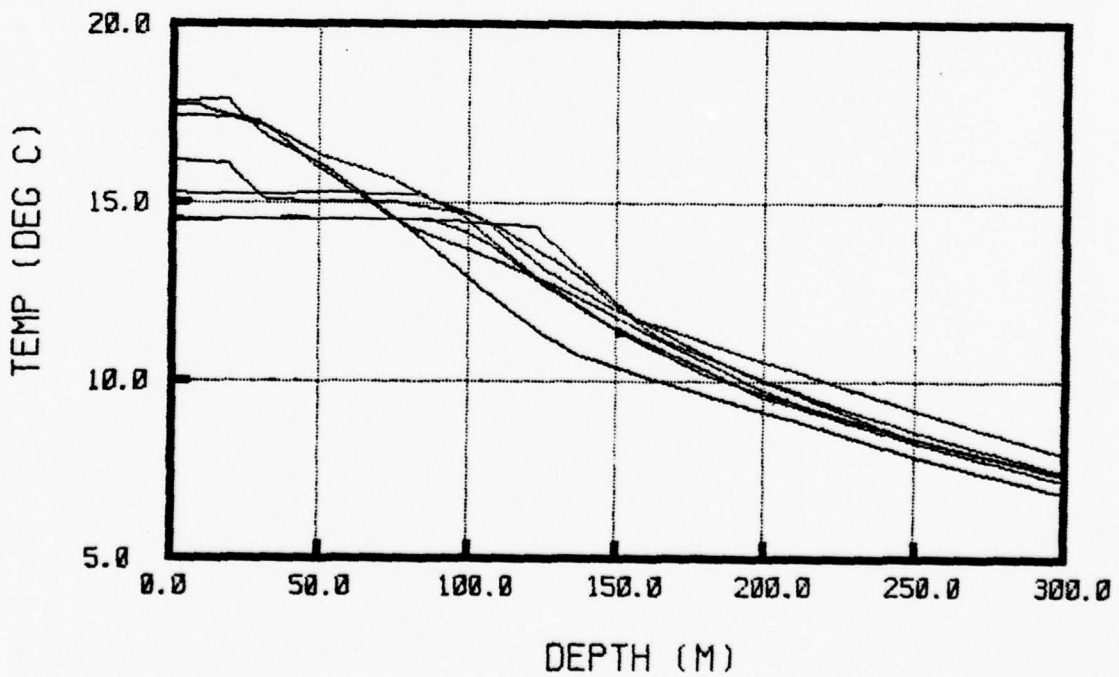
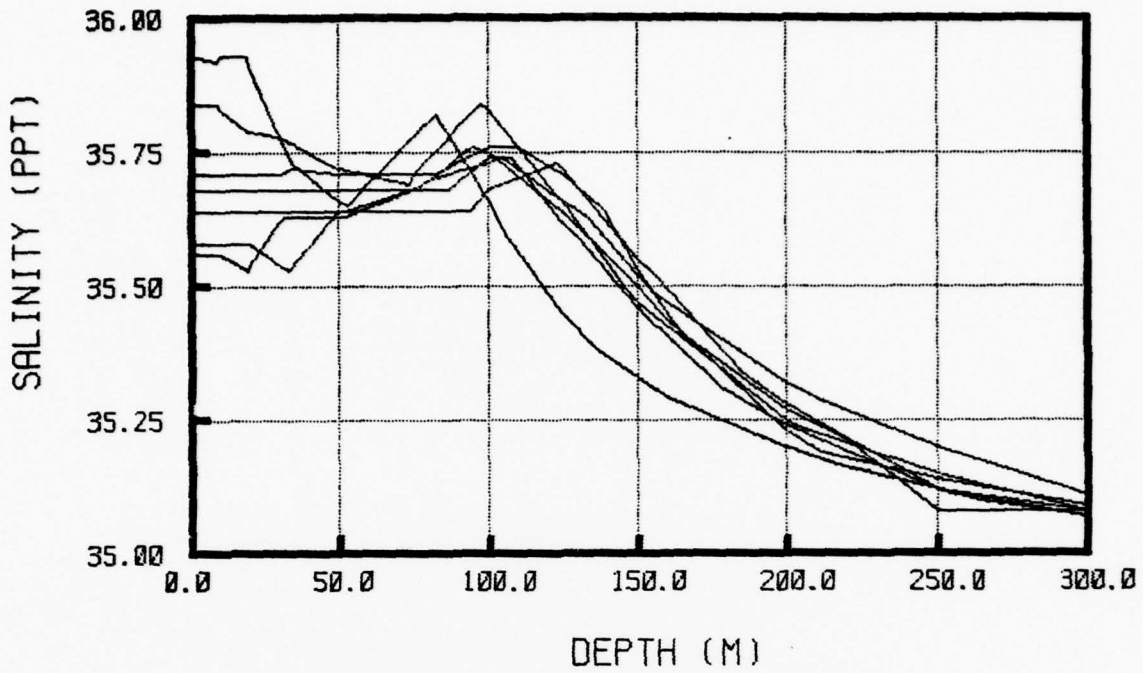


Figure 2. Overplot of hydrocast data for OS HOTEL for the period 21 November-31 December 1974.

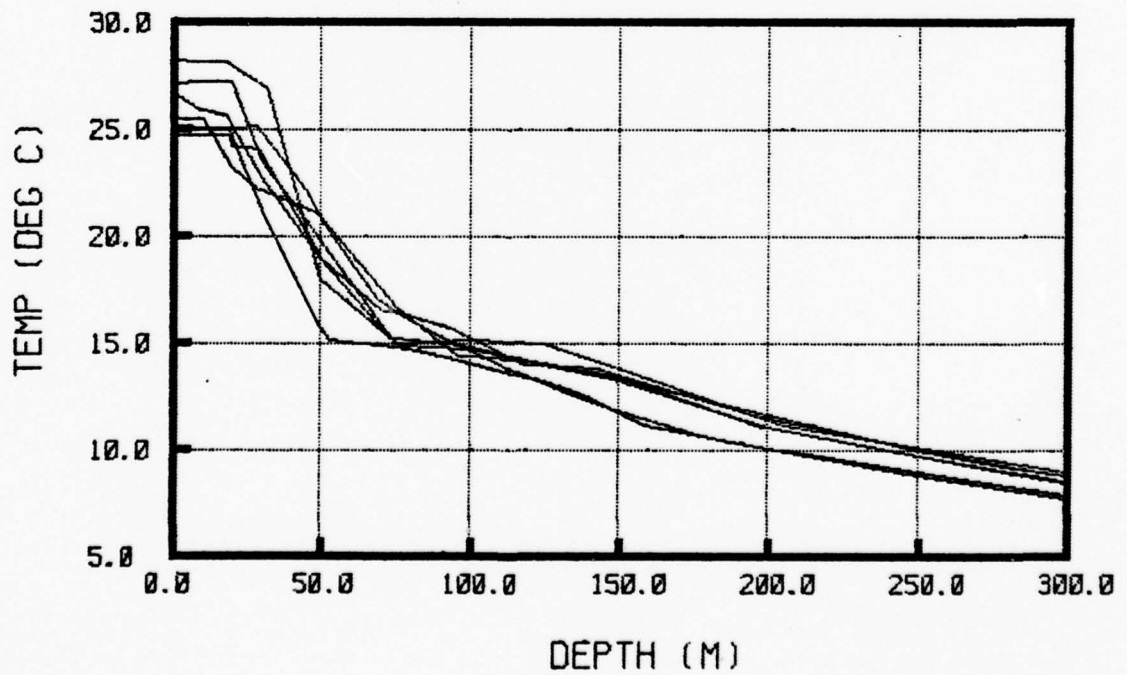
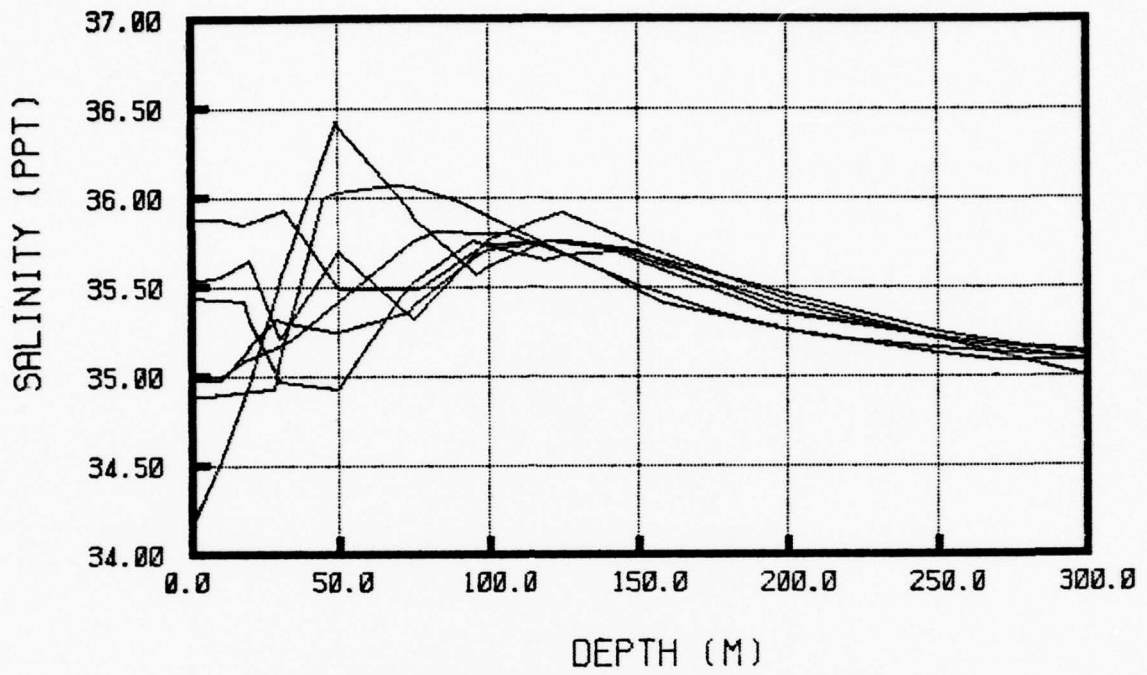


Figure 3. Overplot of hydrocast data for OS HOTEL for the period 8-28 August 1974.

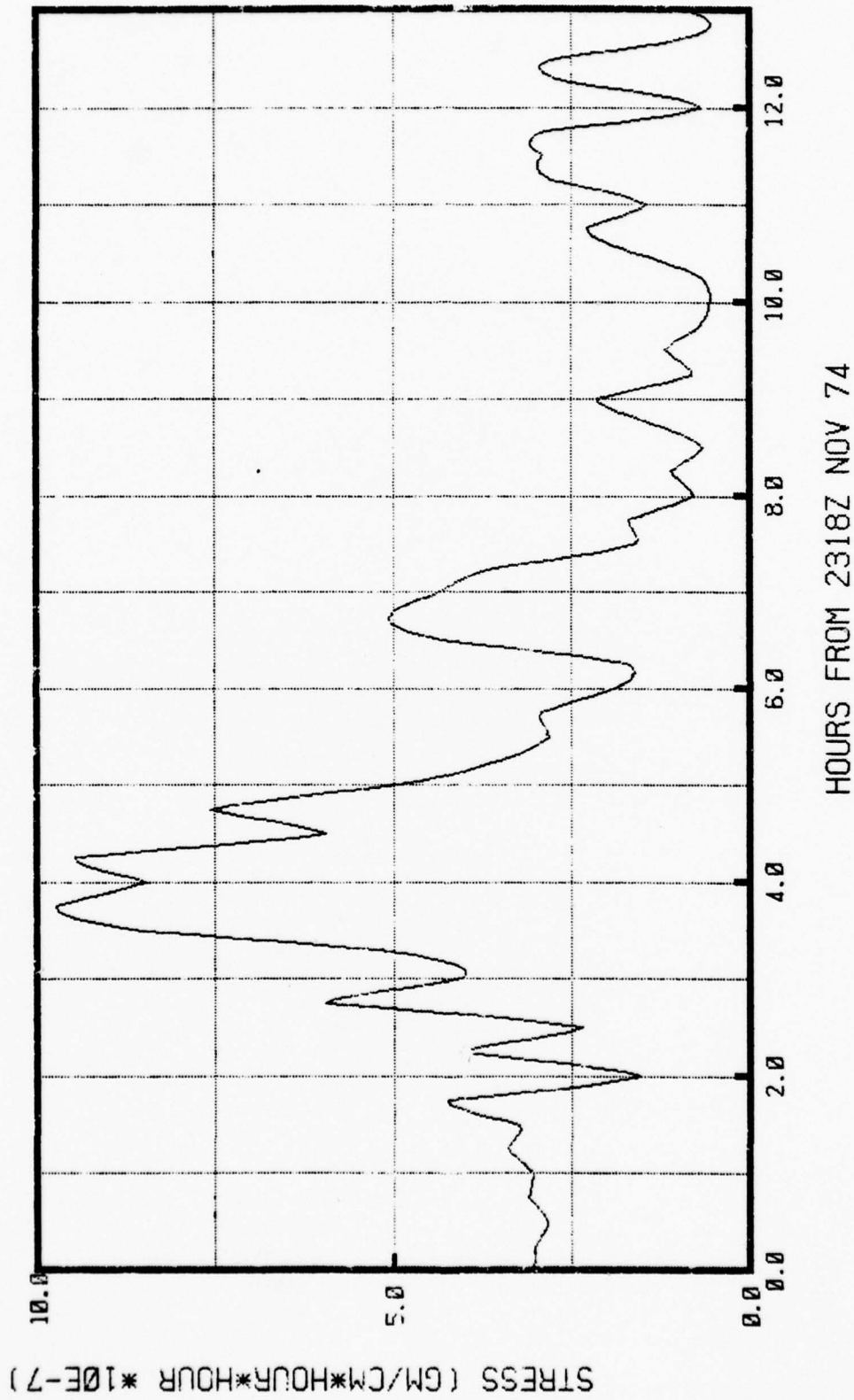


Figure 4. Wind stress at OS PAPA - 18 GMT 23 November to 18 GMT 06 December 1974.

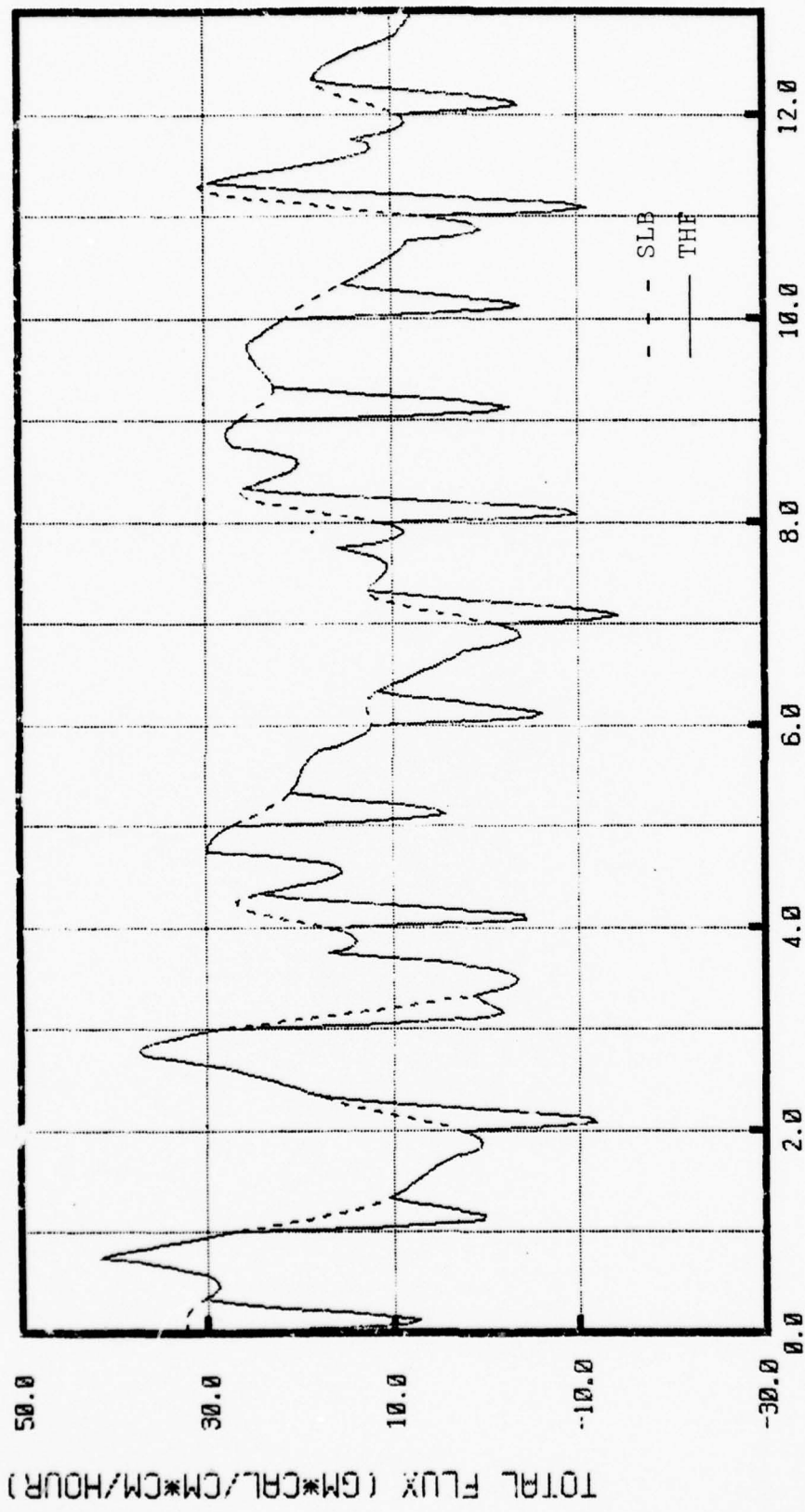


Figure 5. Total heat flux at OS PAPA - 18 GMT 23 November to 18 GMT 06 December 1974. SLB is the sum of sensible and latent heat and back radiation. THF is SLB plus solar radiation.

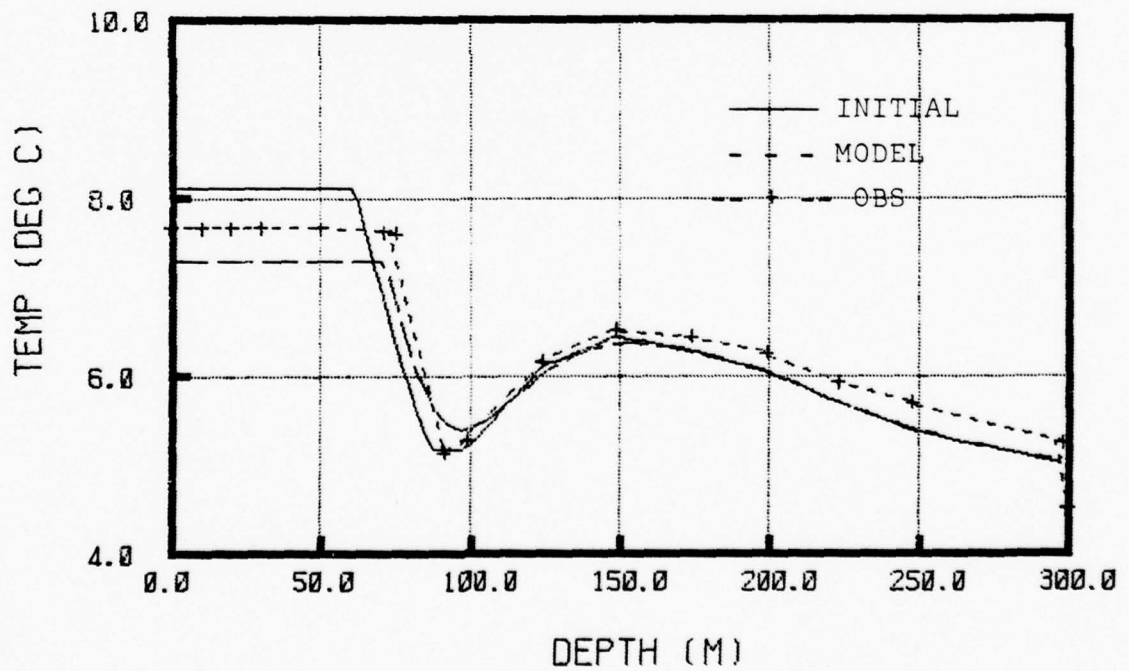
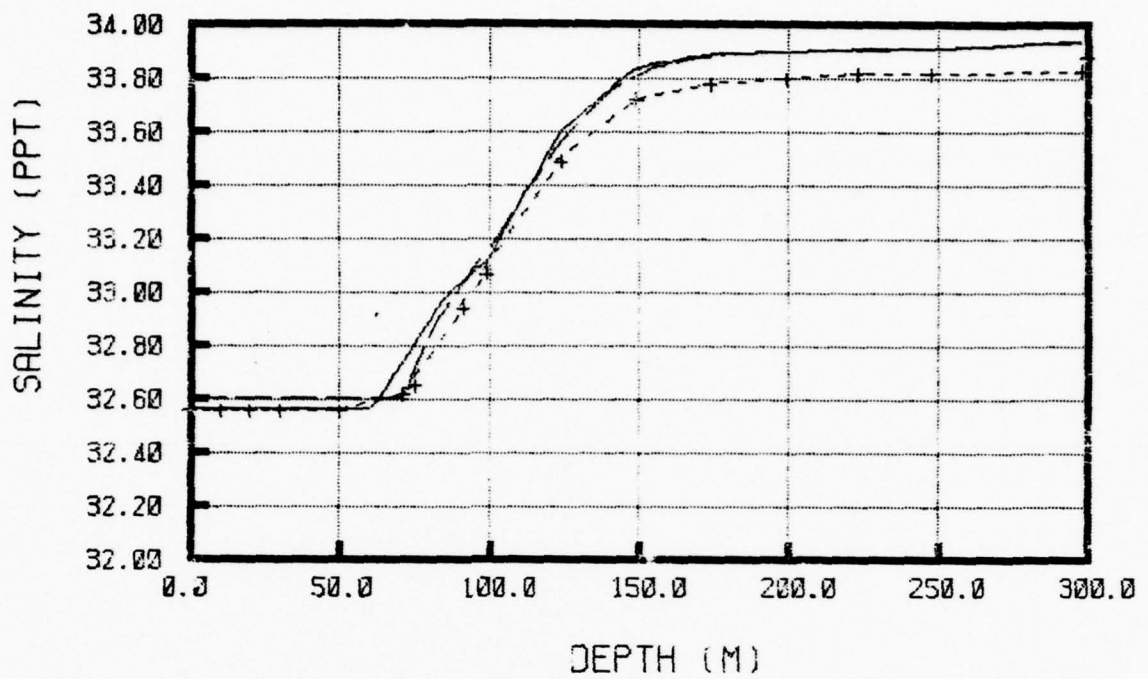


Figure 6. Depth vs temperature and salinity at OS PAPA - 18 GMT 23 November and 18 GMT 06 December 1974, hydrocast data, neglecting (E-P). INITIAL indicates the initialization profiles, MODEL indicates the models predicted profiles, and OBS indicates the observed profiles at the end of the period.

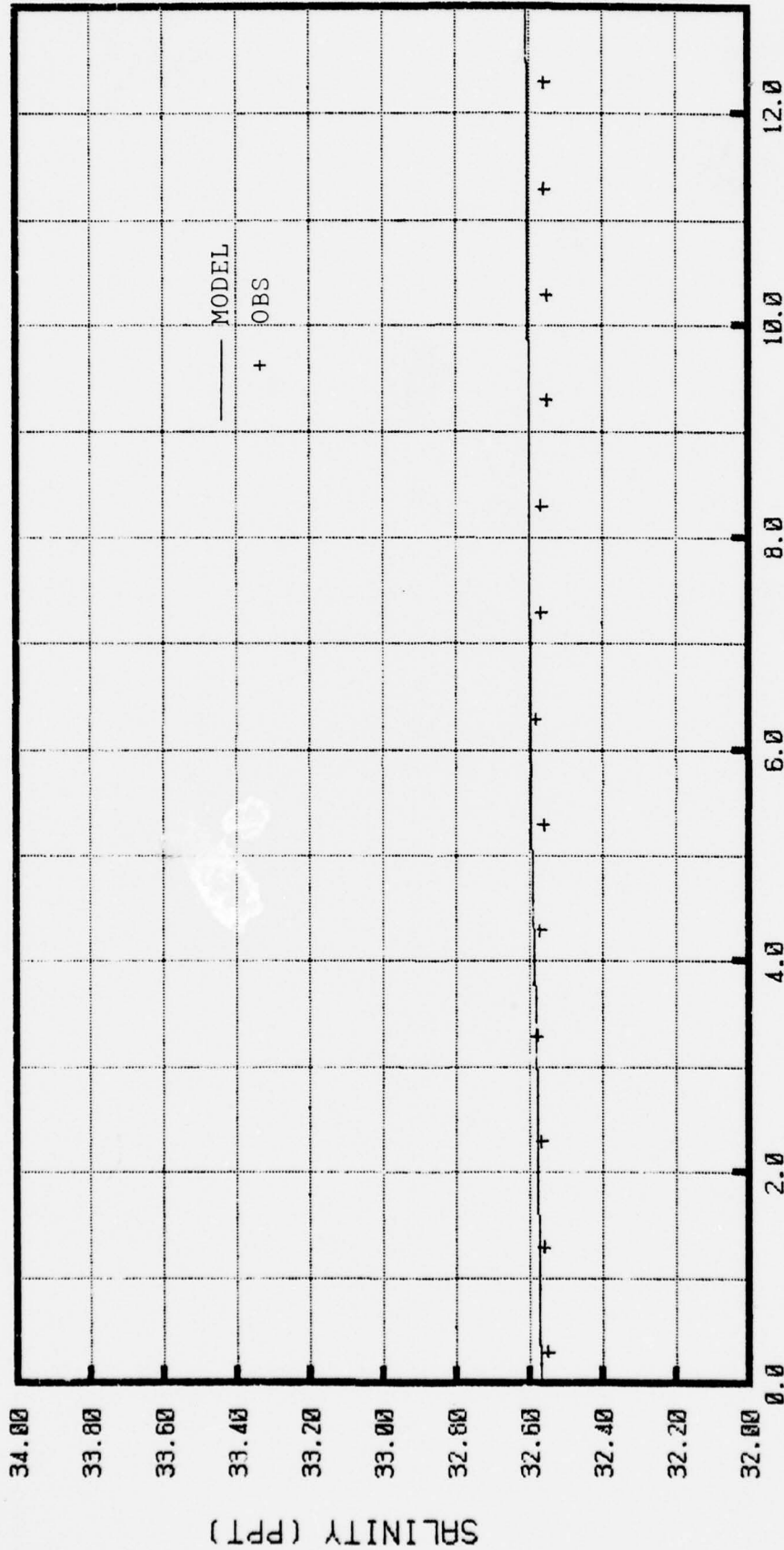
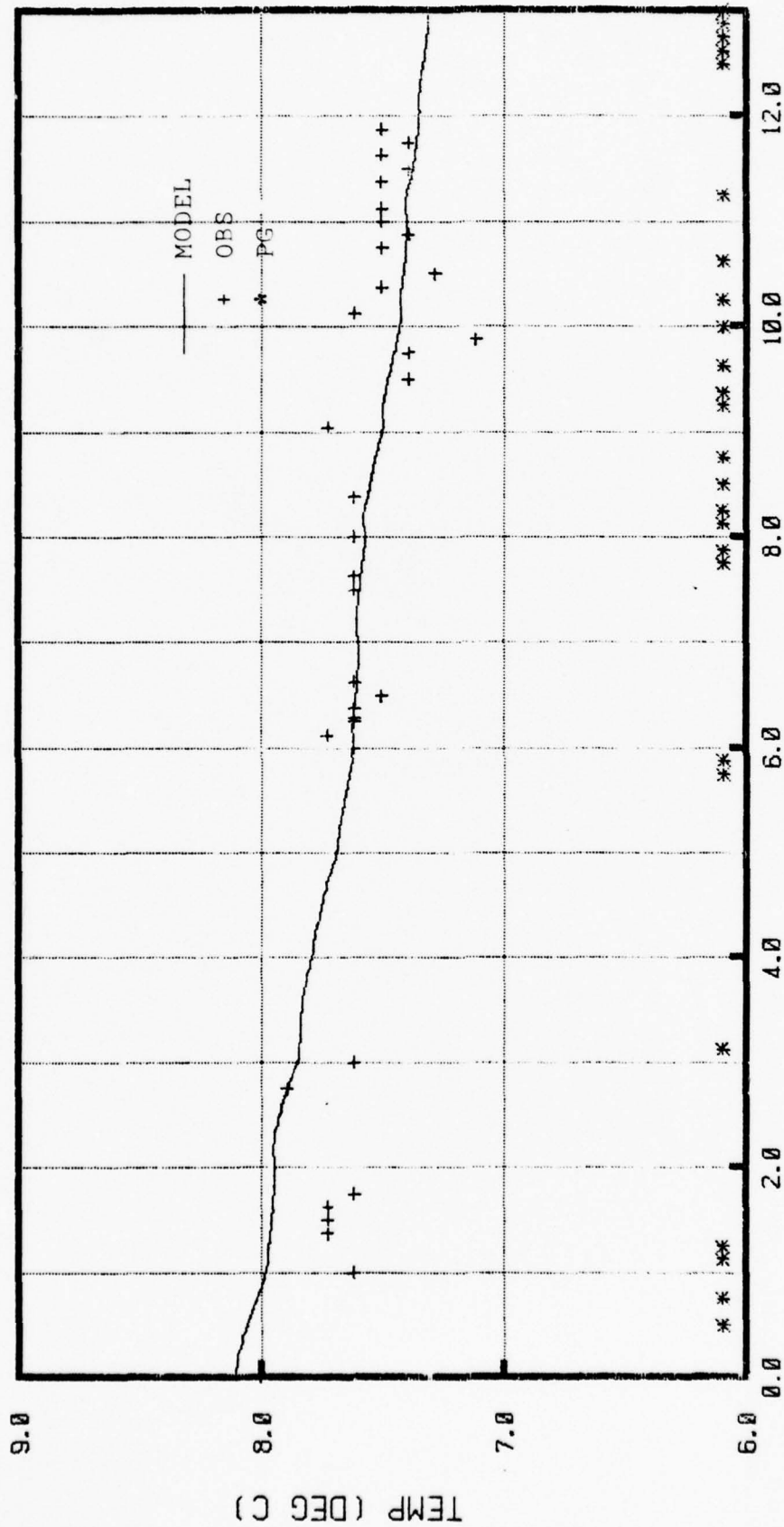
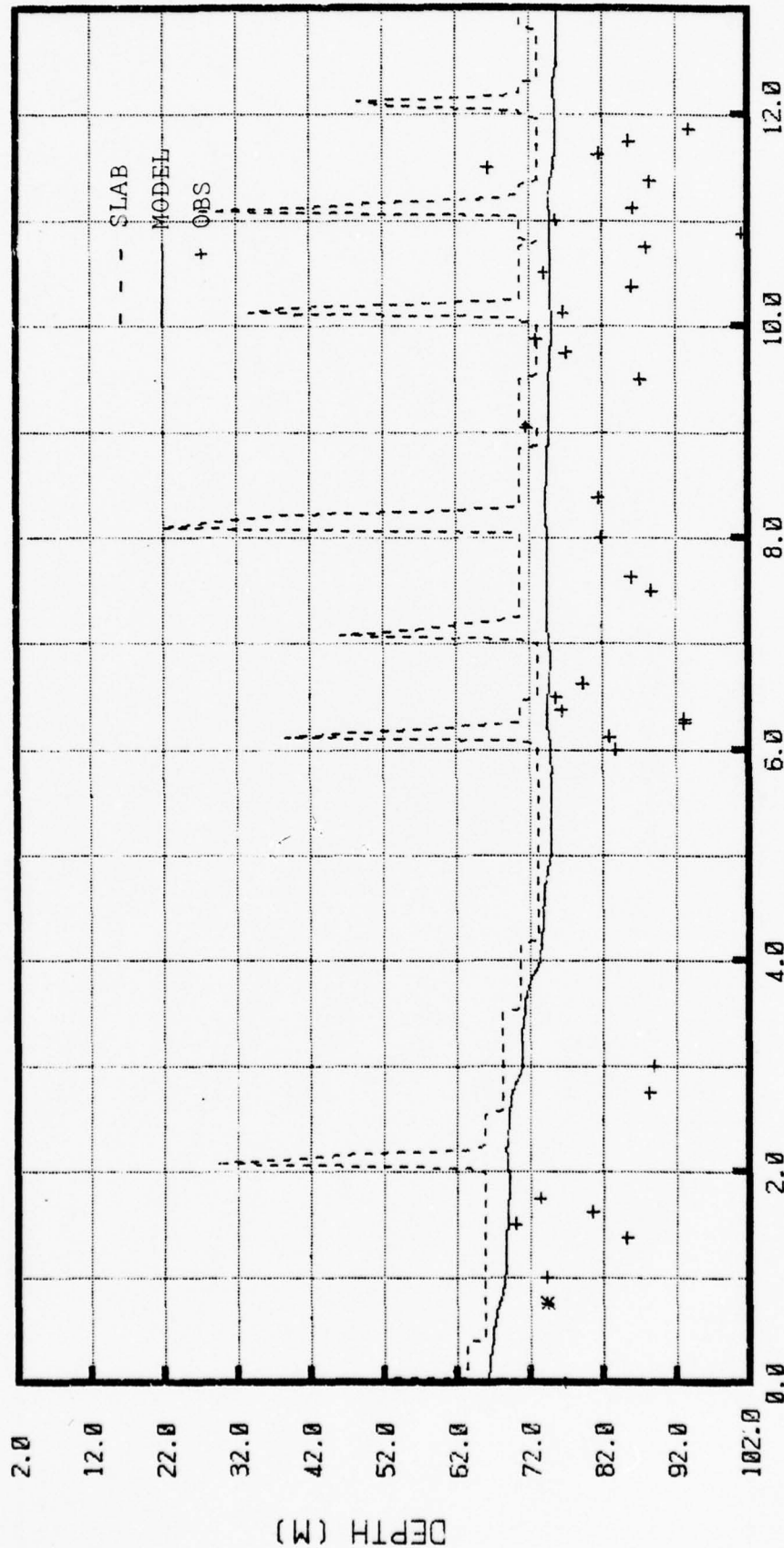


Figure 7. Surface salinity at OS PAPA - 18 GMT 23 November to 18 GMT 06 December 1974, neglecting (E-P). MODEL is the model prediction of salinity and OBS indicate observed values.



DAYS FROM 2318Z NOV 74

Figure 8. Mixed-layer temperature at OS PAPA - 18 GMT 23 November to 18 GMT 06 December 1974 from hydrocast initialization. MODEL indicates predicted temperature, OBS indicate observed values, and PG indicates an observed positive temperature gradient.



DAYS FROM 2318Z NOV 74

Figure 9. Mixed-layer depth at OS PAPA - 18 GMT 23 November to 18 GMT 06 December 1974 from hydrocast initialization. SLAB is the model depth of the isothermal layer, MODEL is the model MLD, and OBS indicates observed values.

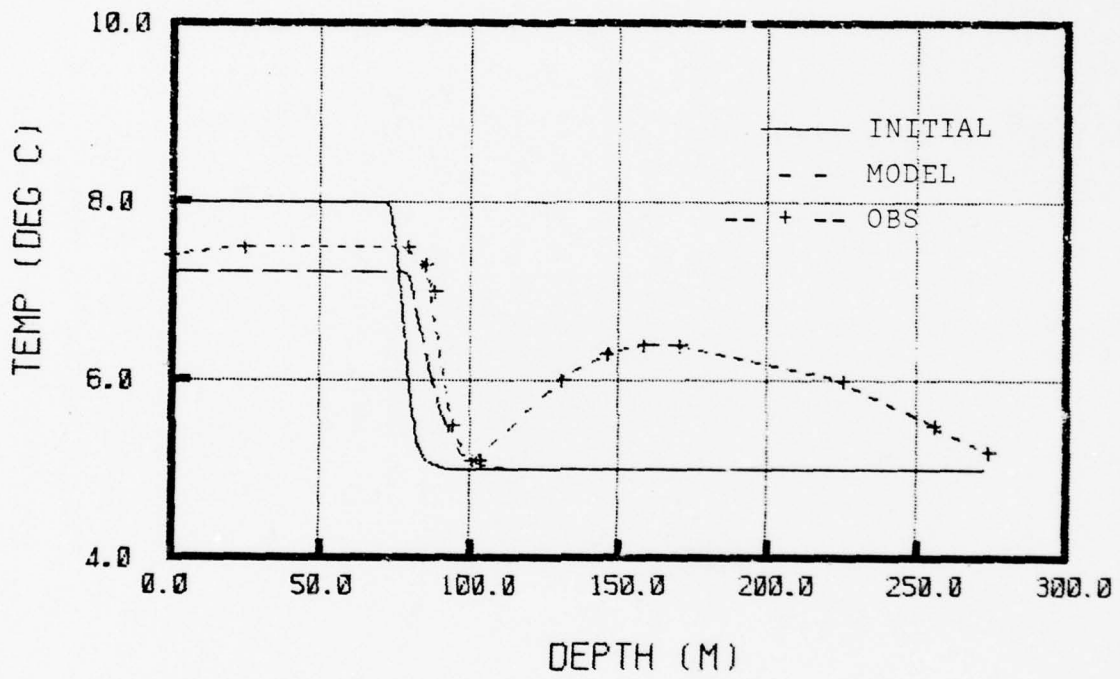
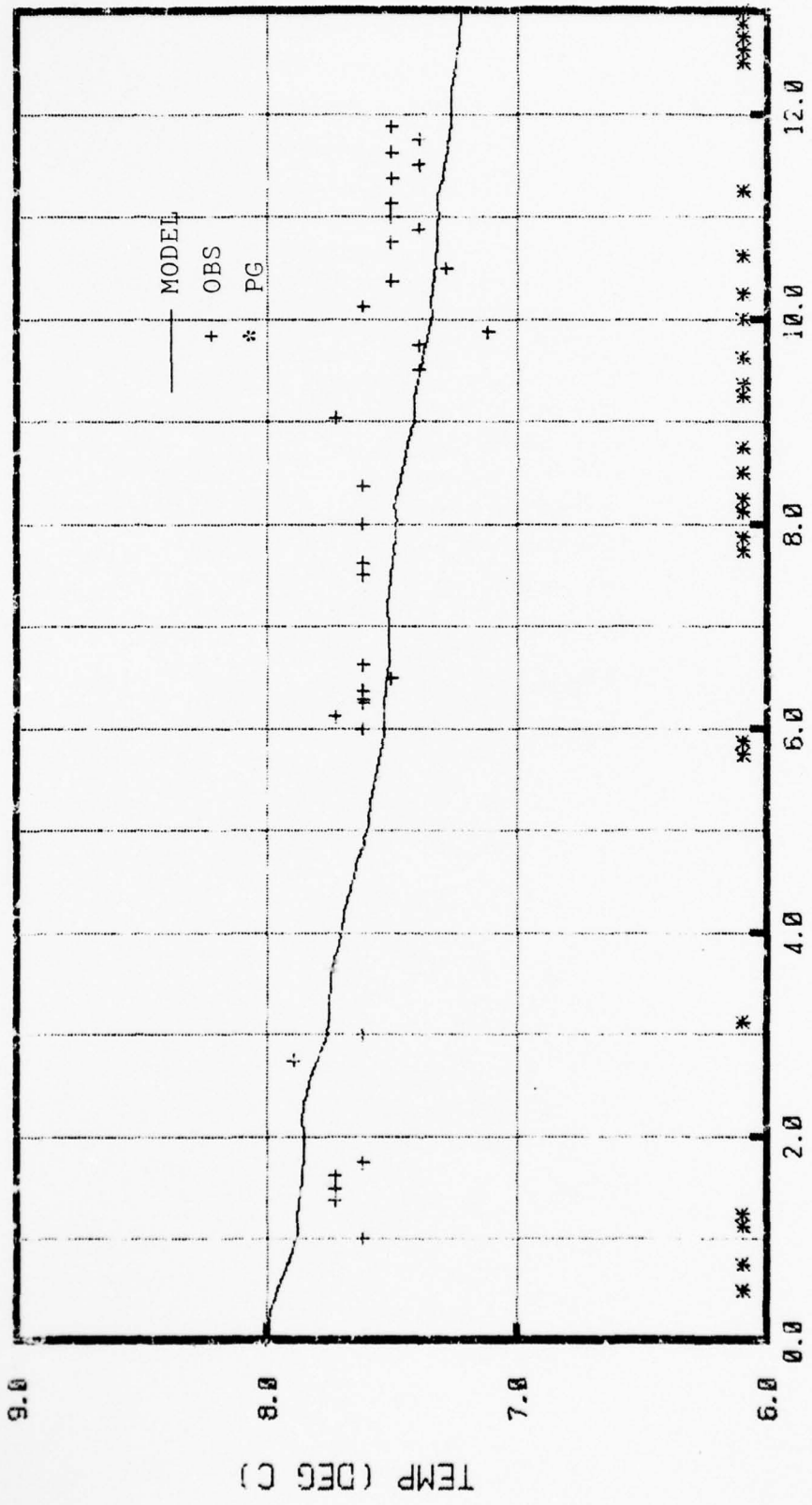
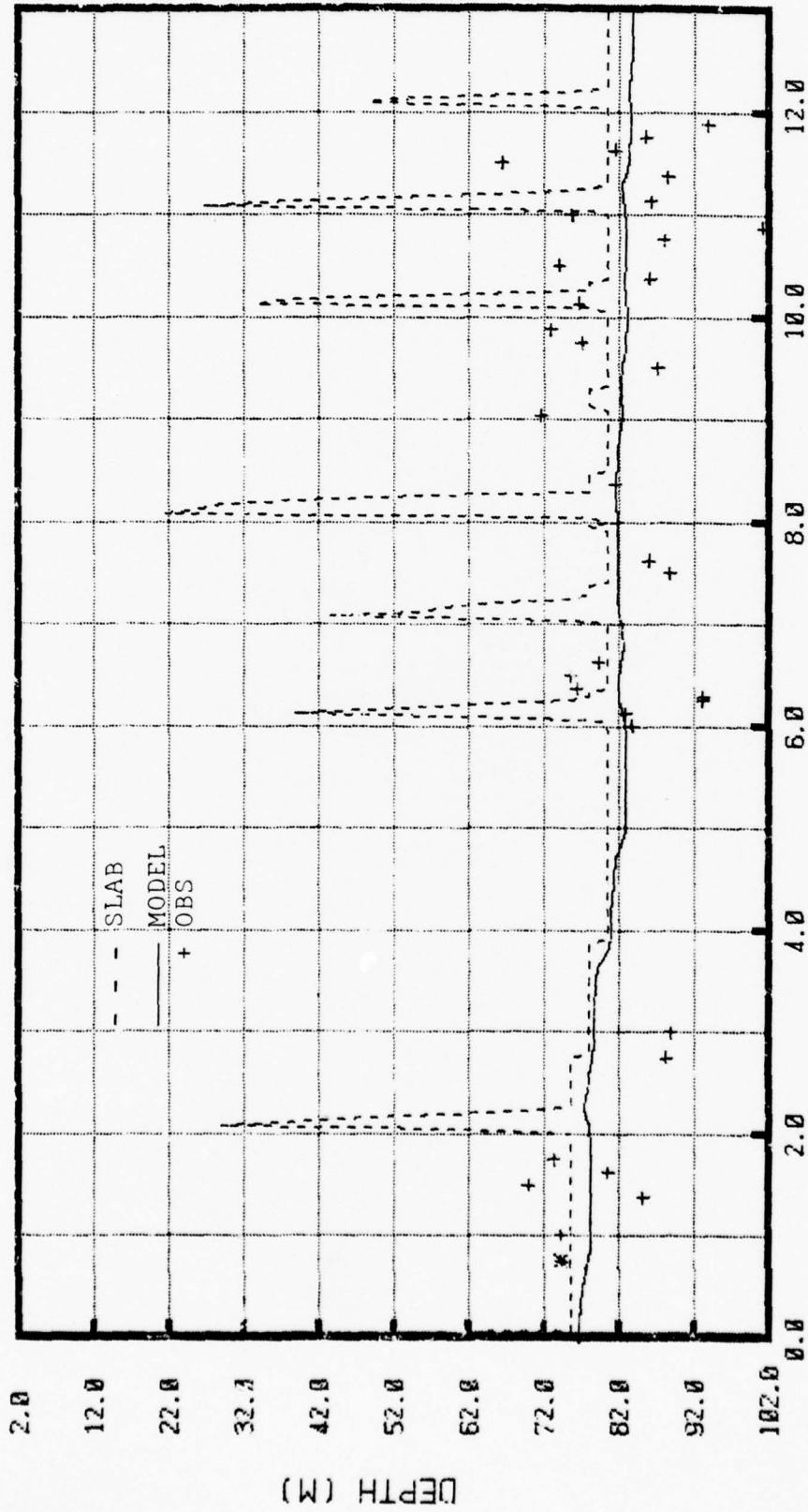


Figure 10. Depth vs temperature at OS PAPA - 18 GMT 23 November and 18 GMT 06 December 1974, BT data.



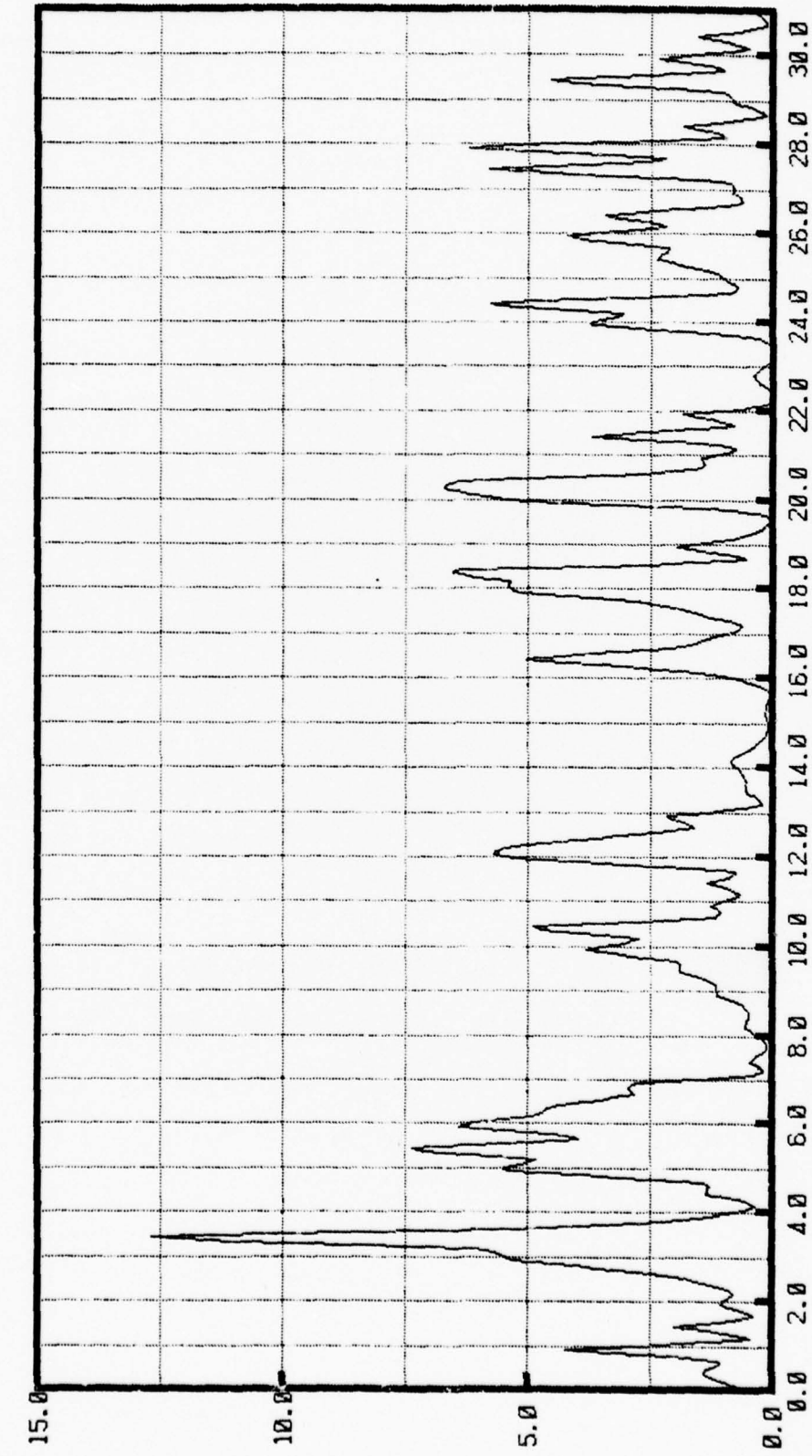
HOURS FROM 2318Z NOV 74

Figure 11. Mixed-layer temperature at OS PAPA - 18 GMT 23 November to 18 GMT 06 December 1974 from BT initialization.



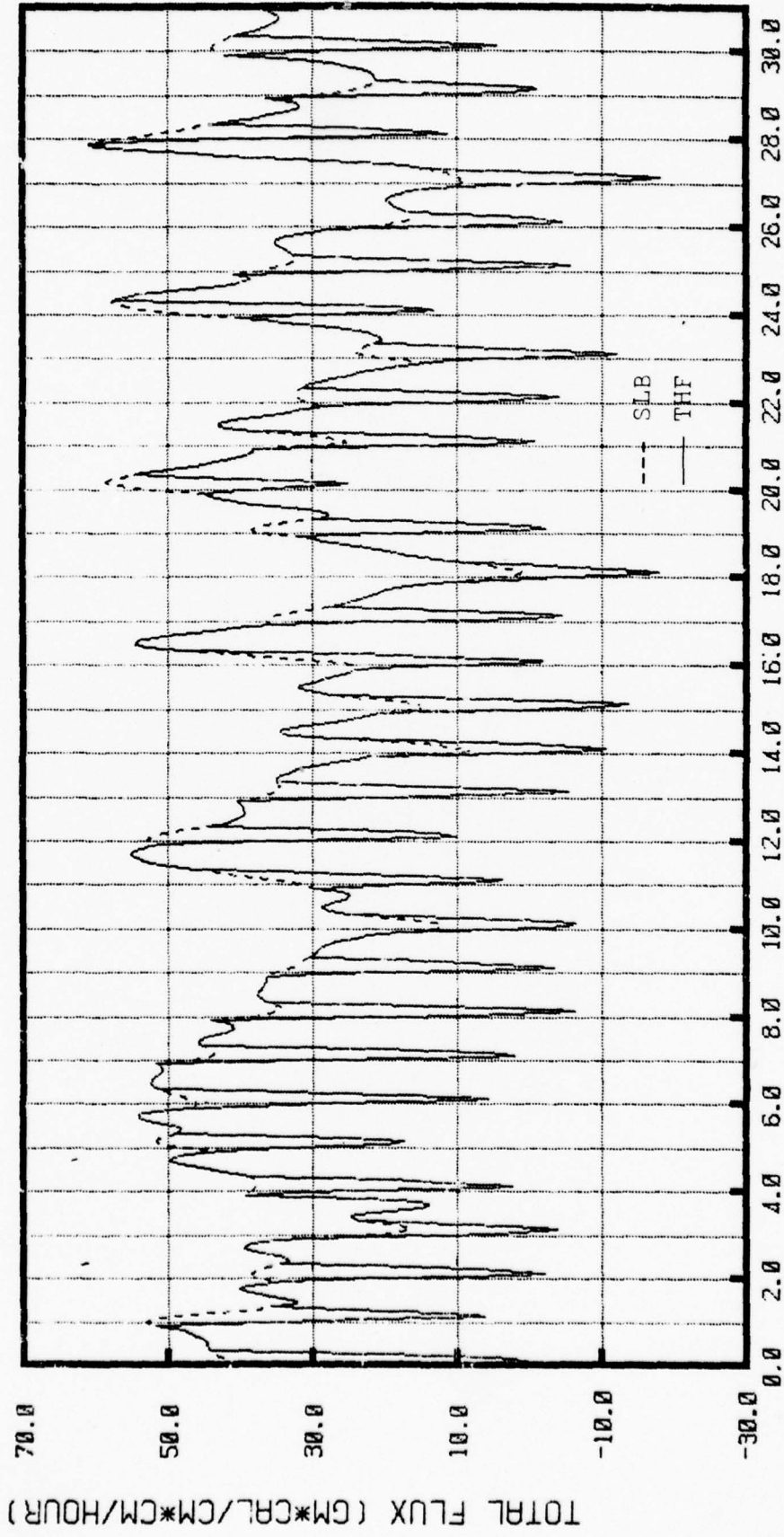
HOURS FROM 2318Z NOV 74

Figure 12. Mixed-layer depth at OS PAPA - 18 GMT 23 November to 18 GMT 06 December 1974 from BT initialization.



DAYS FROM 2814Z NOV 74

Figure 13. Wind stress at OS HOTEL - 14 GMT 28 November to 14 GMT 29 December 1974.



DAYS FROM 2814Z NOV 74

Figure 14. Total heat flux at OS HOTEL - 14 GMT 28 November to 14 GMT 29 December 1974.

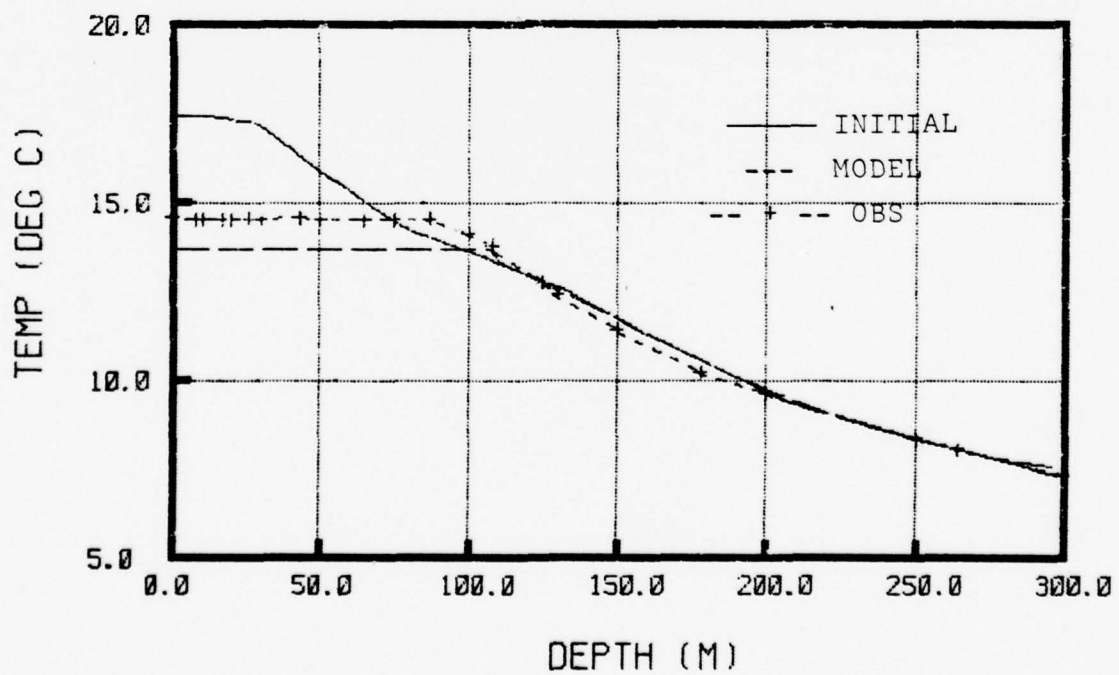
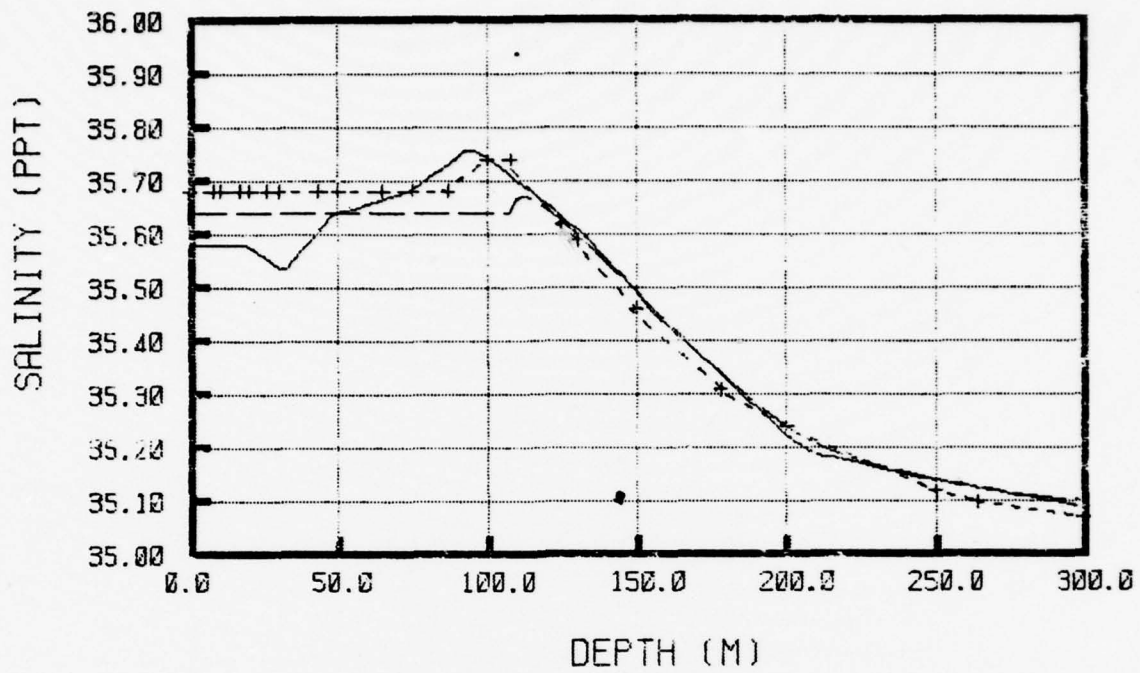
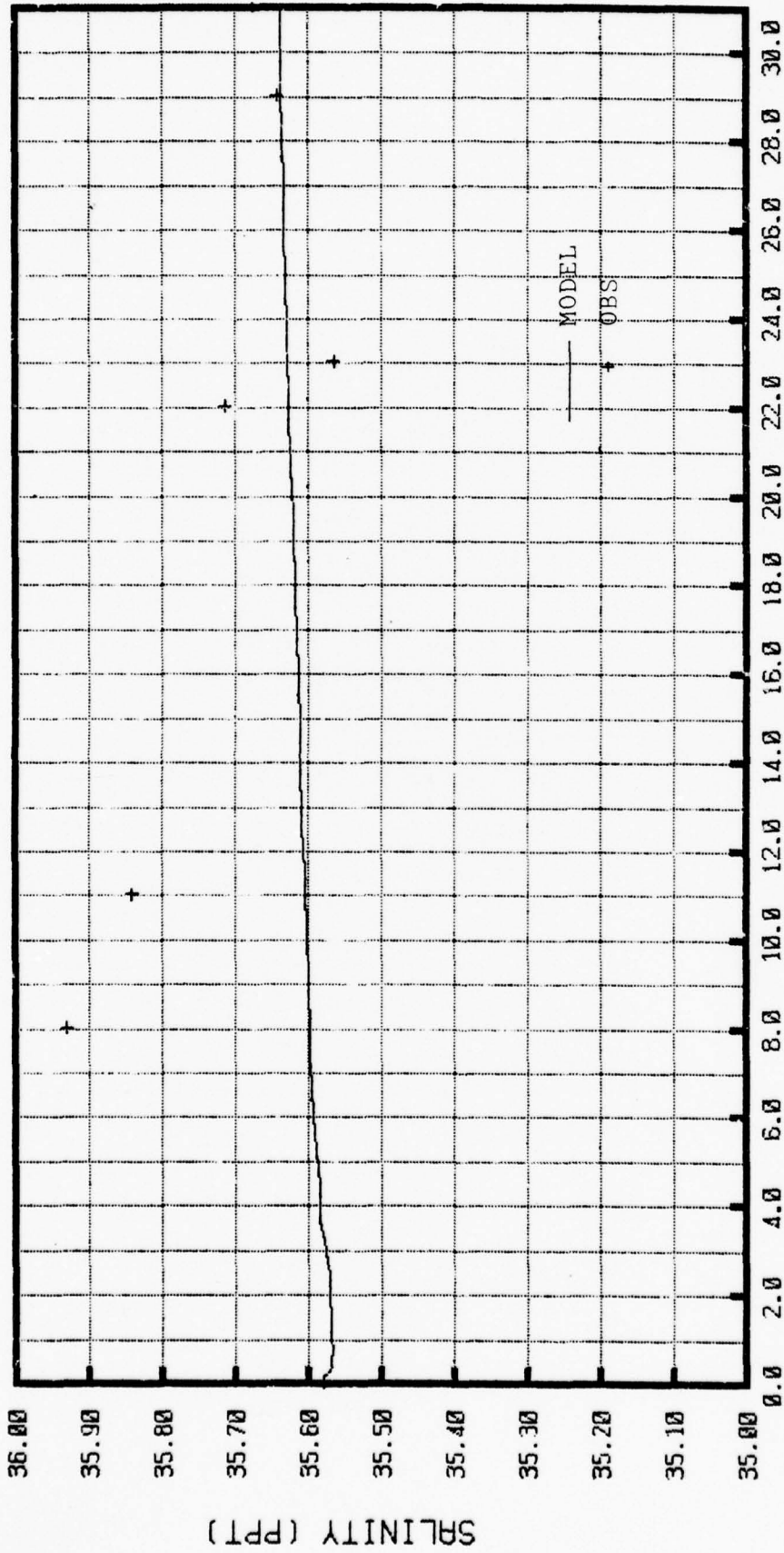
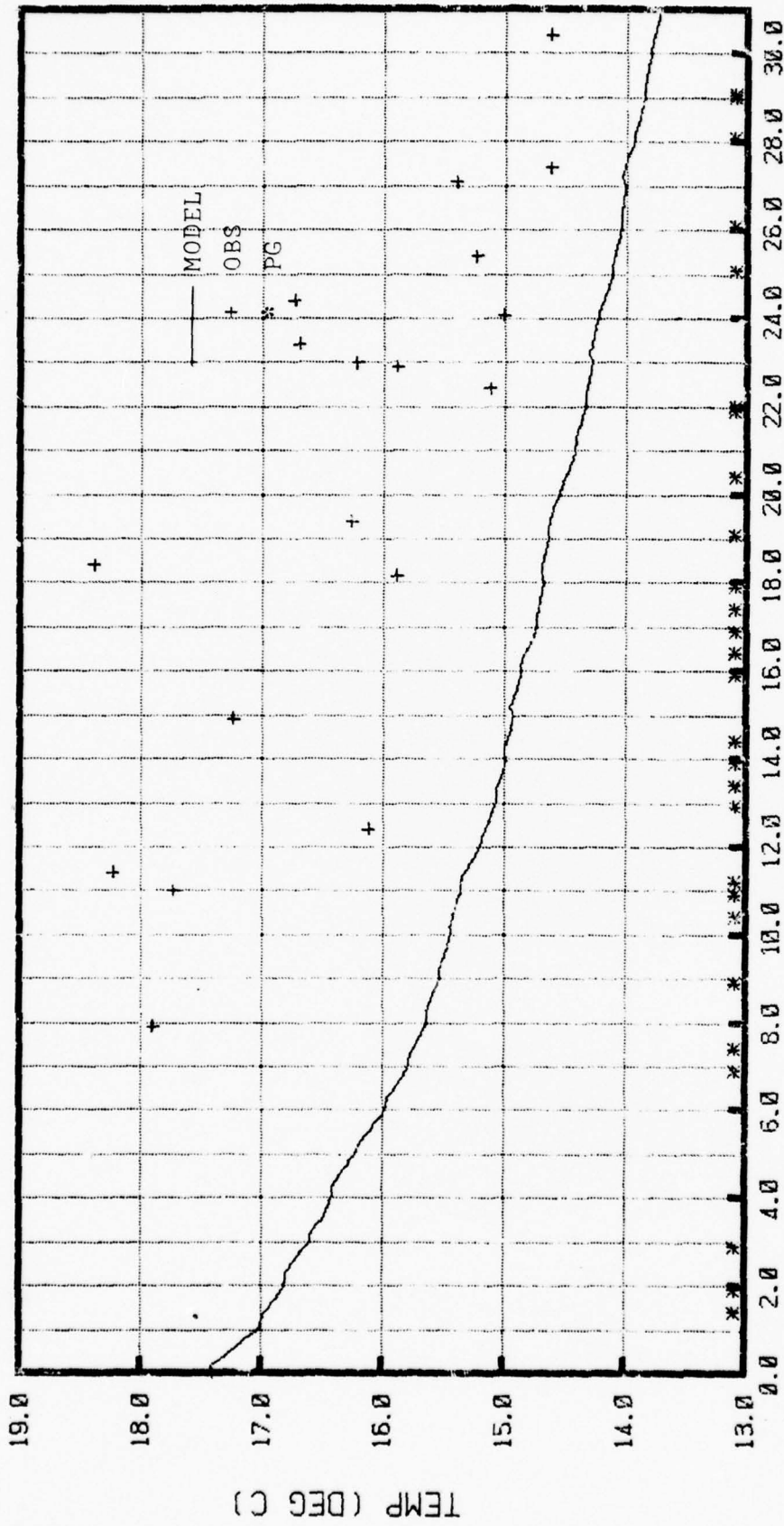


Figure 15. Depth vs temperature and salinity at OS HOTEL - 14 GMT 28 November and 14 GMT 29 December 1974, hydrocast data, neglecting (E-P).



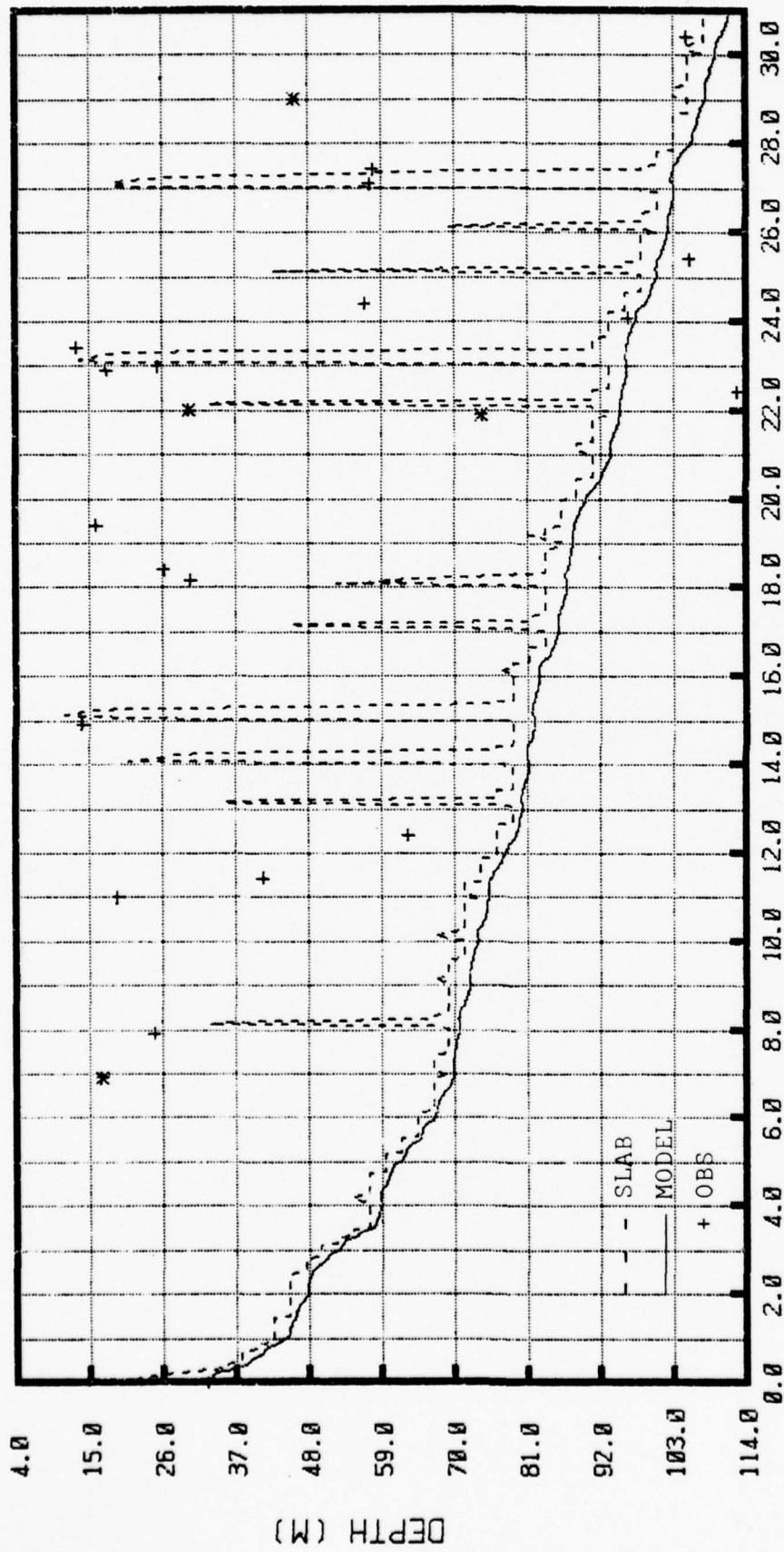
DAYS FROM 2814Z NOV 74

Figure 16. Surface salinity at OS HOTEL - 14 GMT 28 November to 14 GMT 29 December 1974, neglecting (E-P).



DAYS FROM 2814Z NOV 74

Figure 17. Mixed-layer temperature at OS HOTEL - 14 GMT 28 November to 14 GMT 29 December 1974 from hydro-cast initialization.



DAYS FROM 2814Z NOV 74

Figure 18. Mixed-layer depth at OS HOTEL - 14 GMT 28 November to 14 GMT 29 December 1974 from hydrocast initialization.

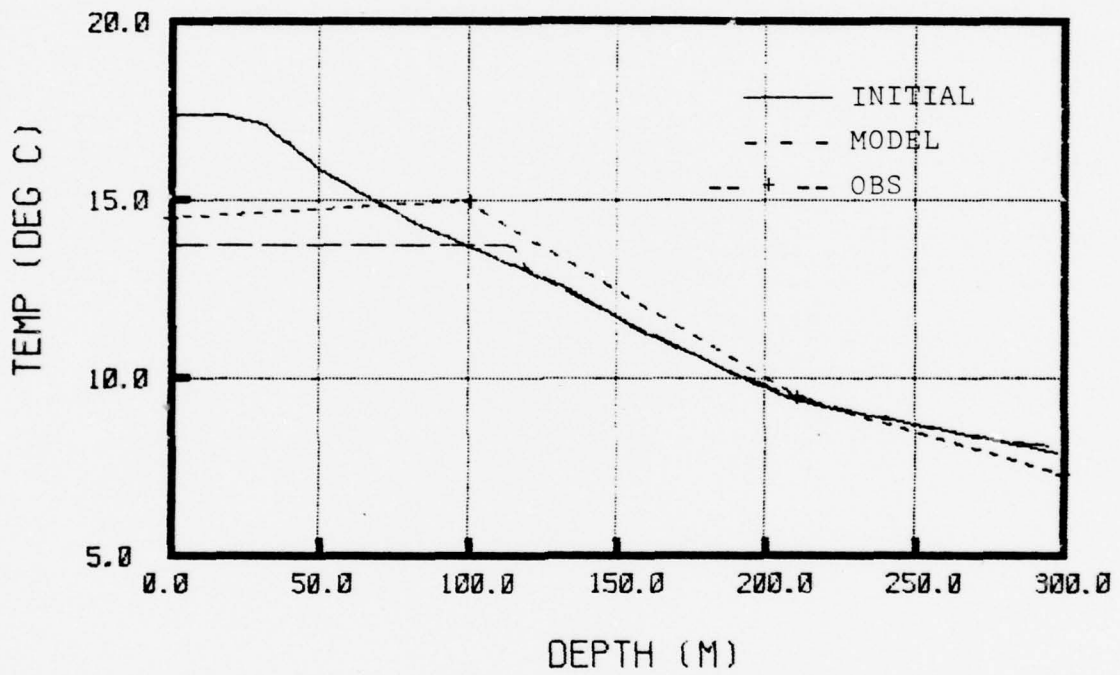
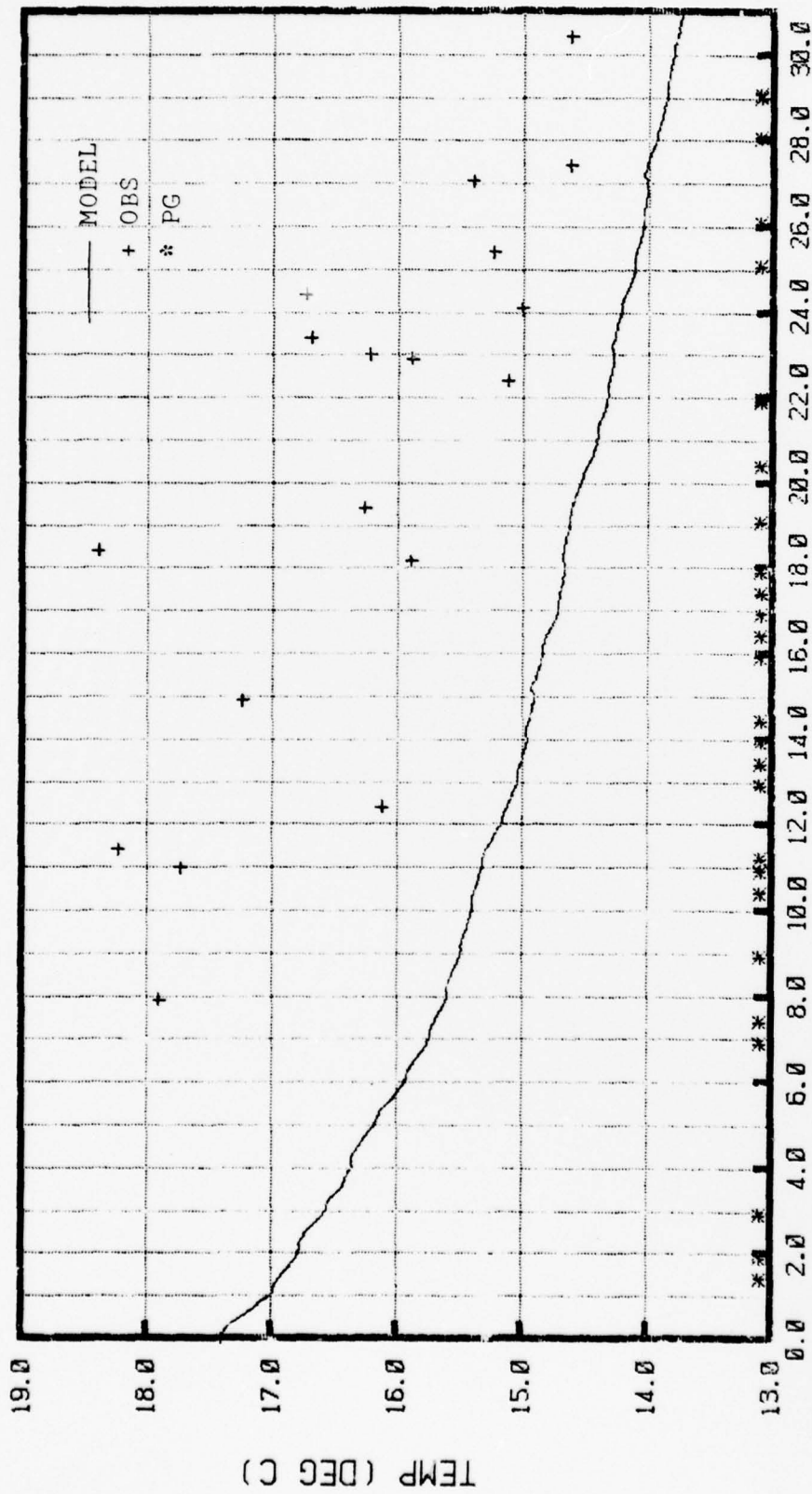
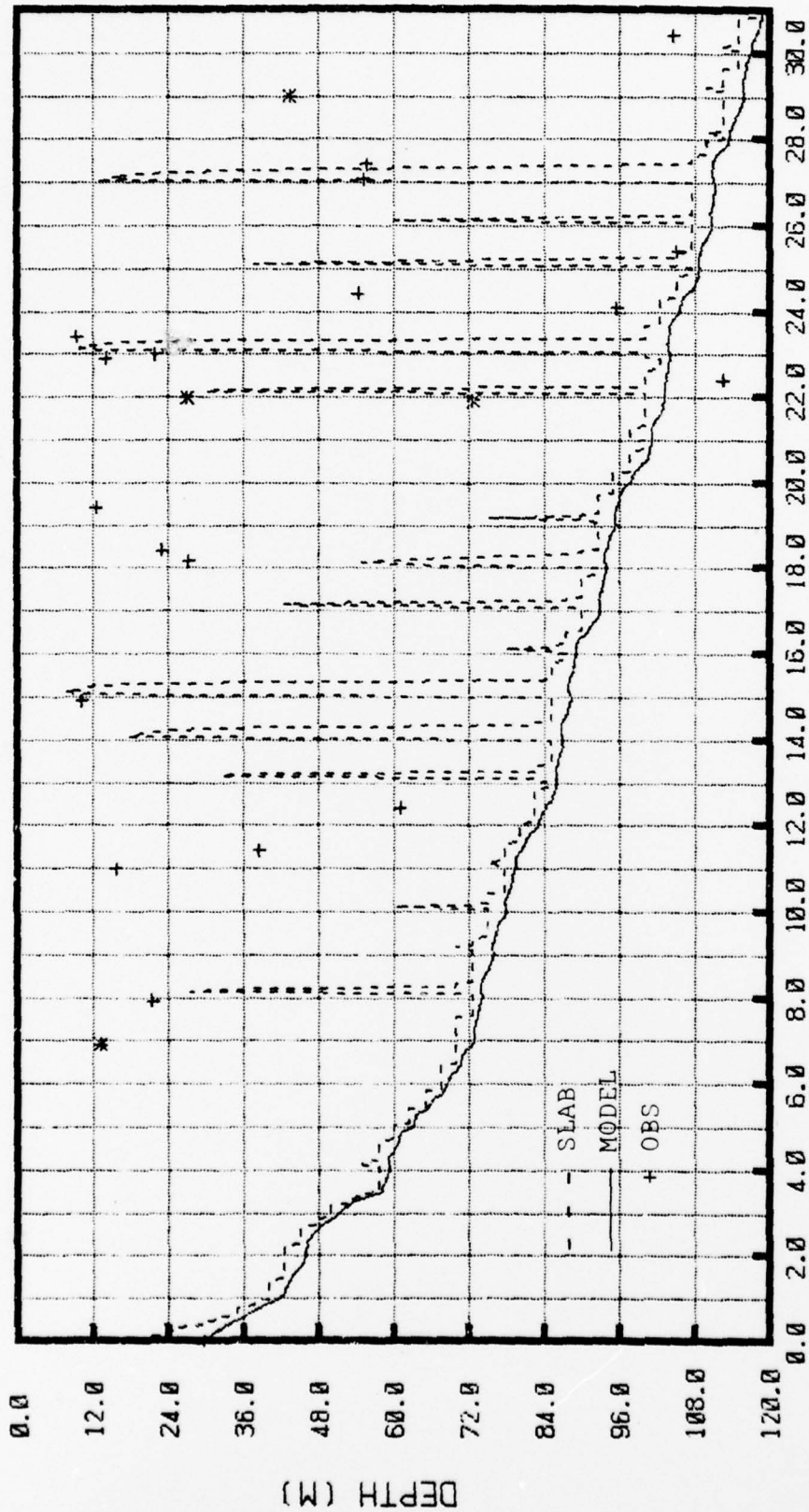


Figure 19. Depth vs temperature at OS HOTEL - 14 GMT 28 November and 14 GMT 29 December, BT data.



HOURS FROM 2814Z NOV 74

Figure 20. Mixed-layer temperature at OS HOTEL - 14 GMT 28 November to 14 GMT 29 December 1974 from BT initialization.



HOURS FROM 2814Z NOV 74

Figure 21. Mixed-layer depth at OS HOTEL - 14 GMT 28 November to 14 GMT 29 December 1974 from BT initialization.

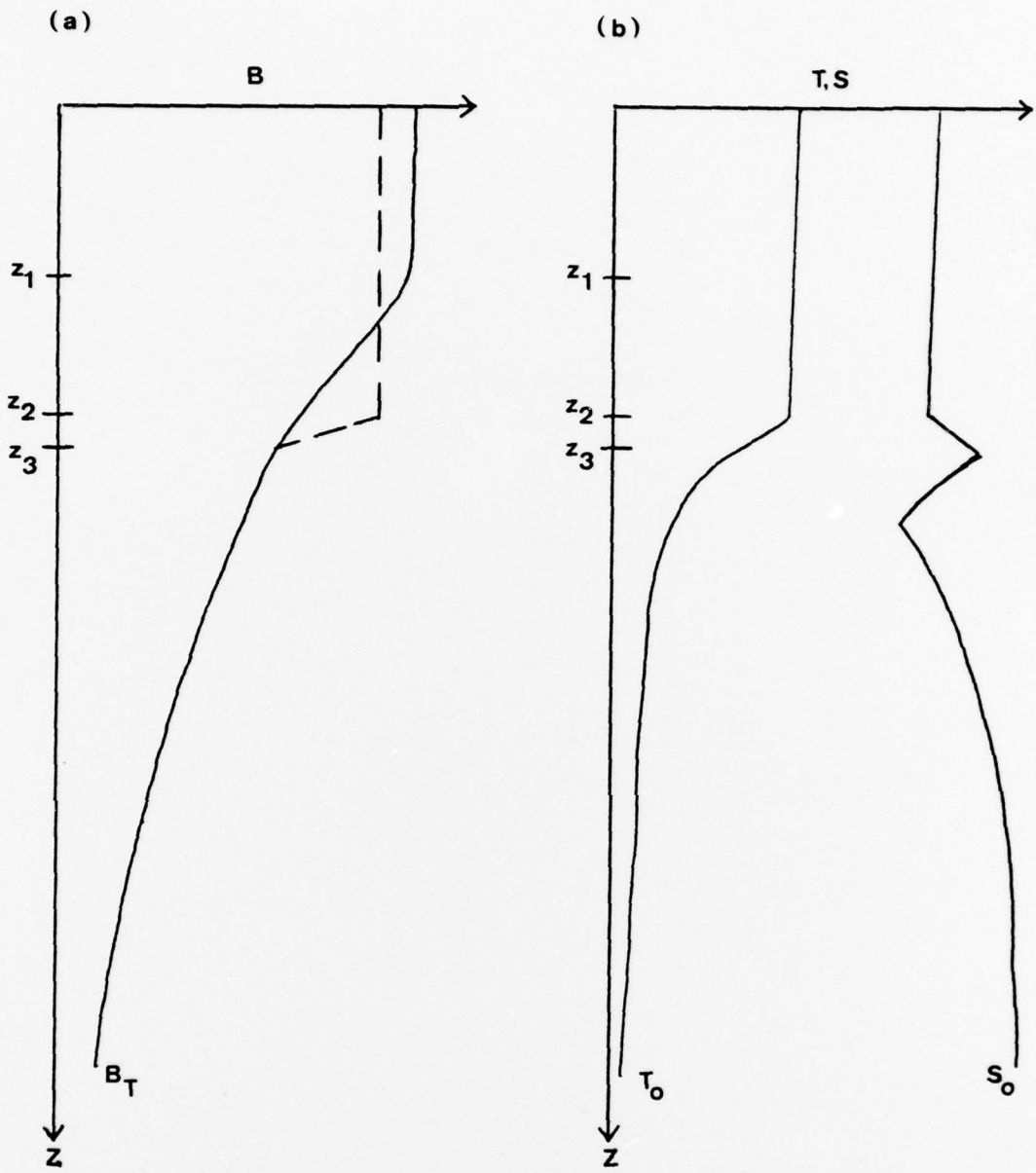


Figure 22. Schematic of a derived salinity profile assuming a typical buoyancy.

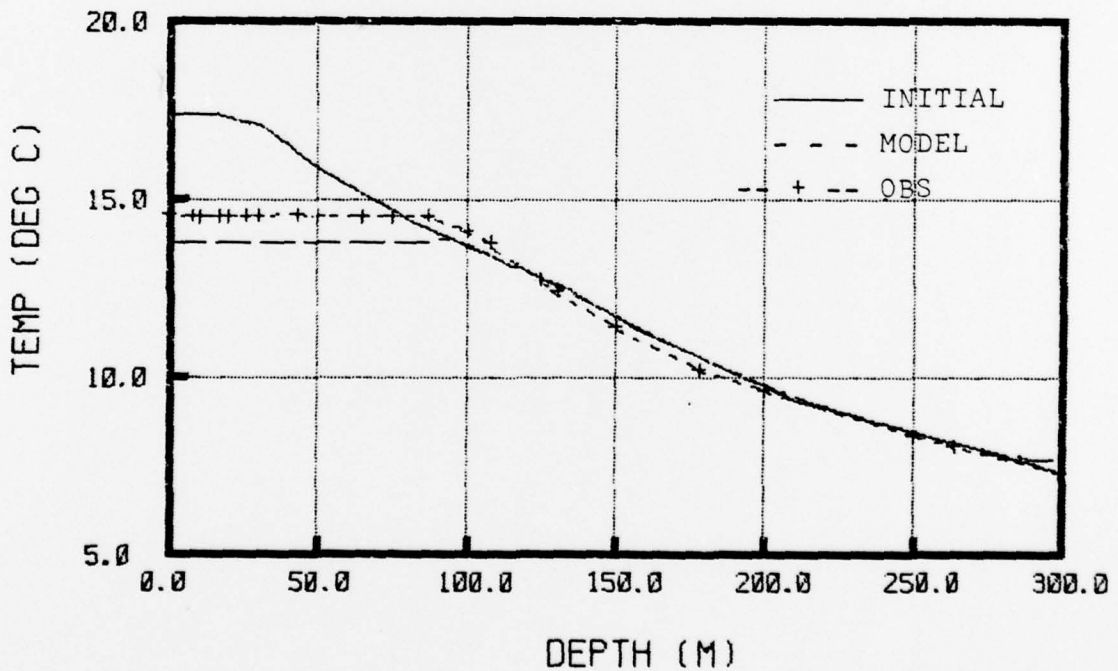
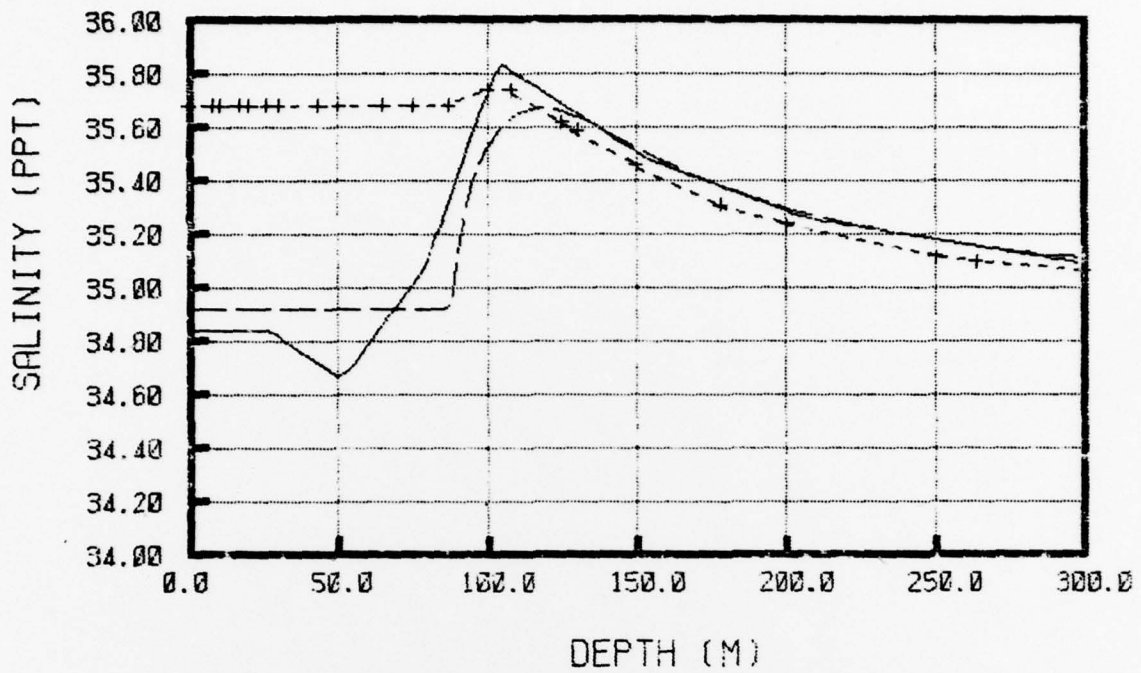
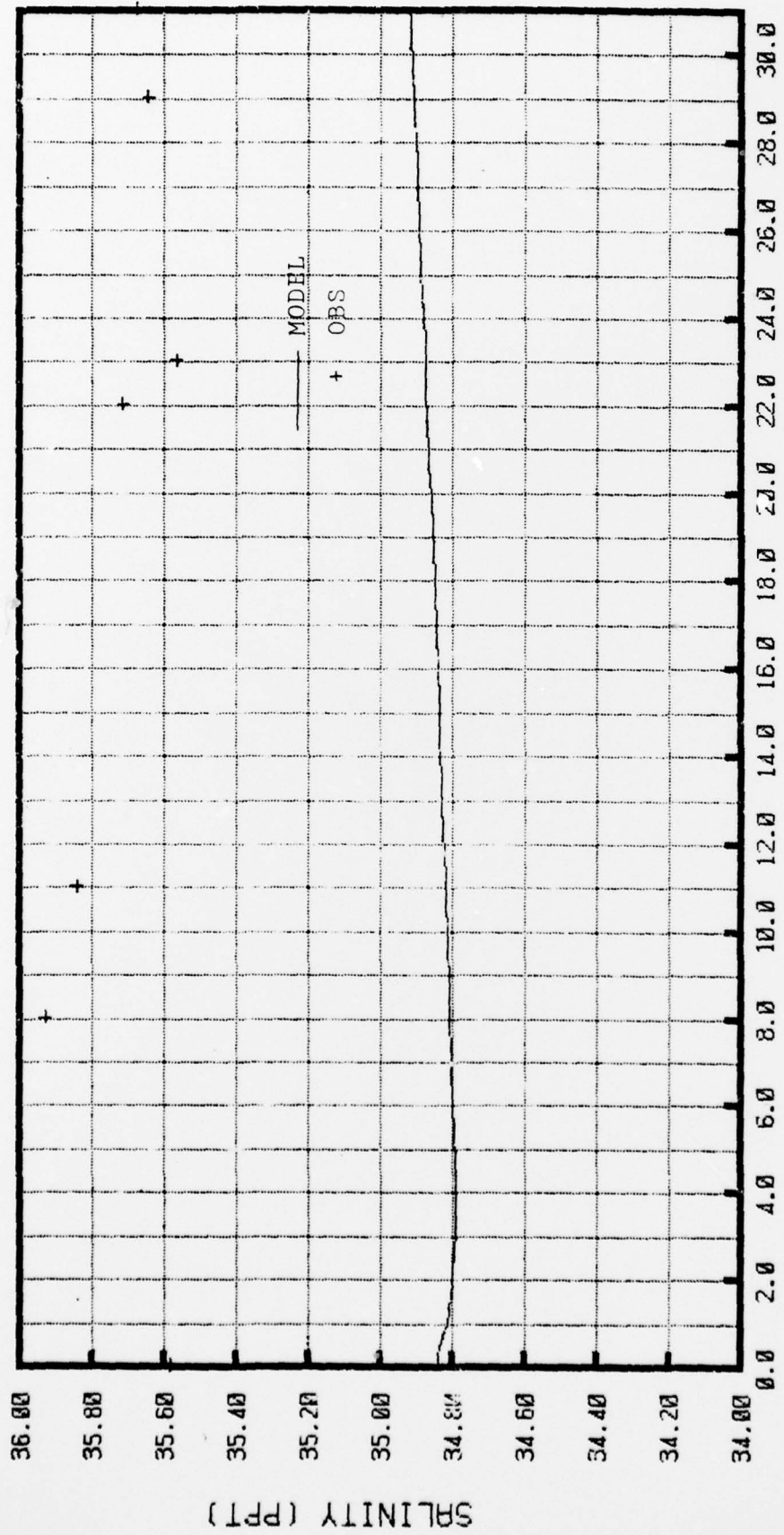
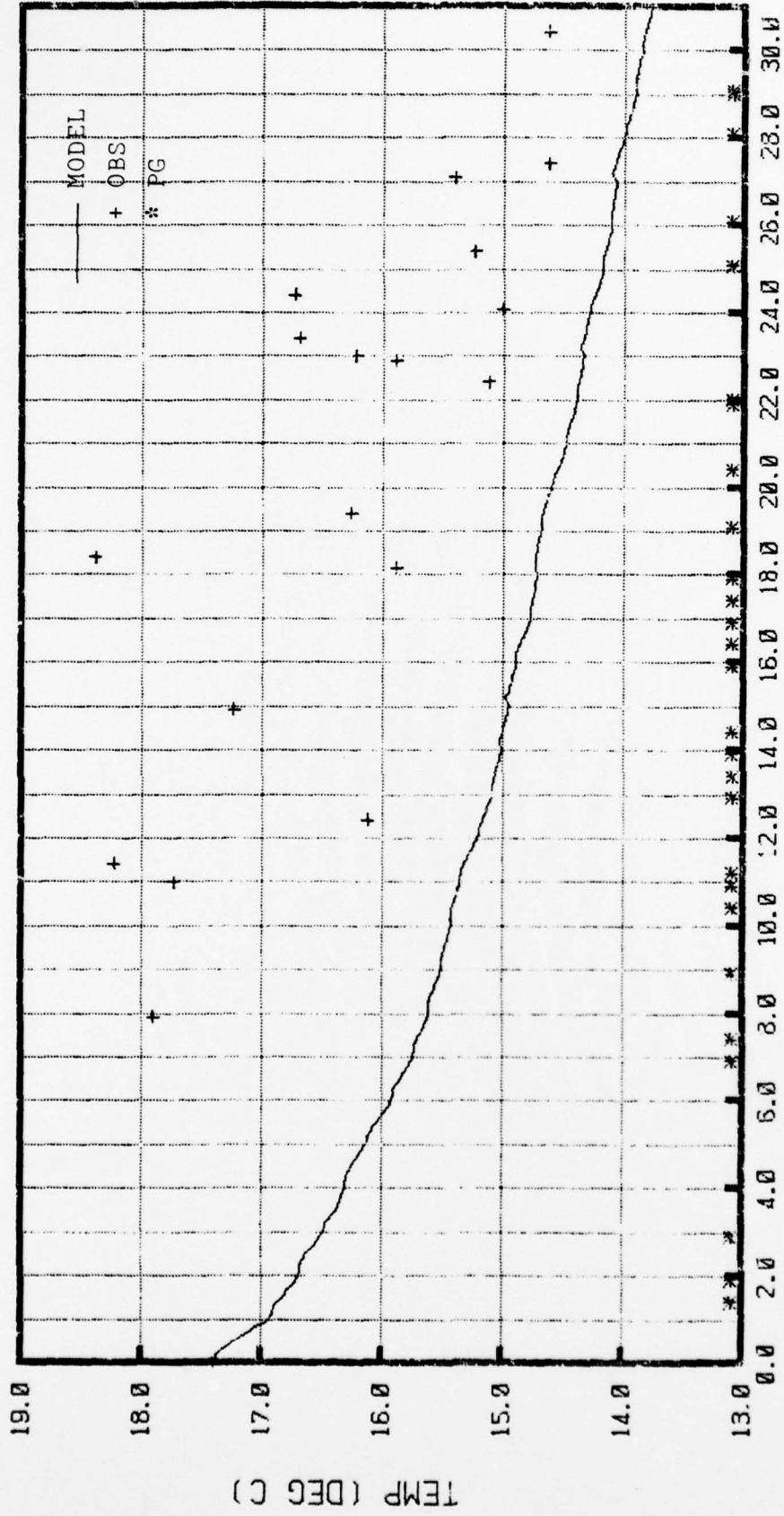


Figure 23. Depth vs temperature and salinity at OS HOTEL - 14 GMT 28 November and 14 GMT 29 December 1974, BT and typical salinity data, neglecting (E-P).



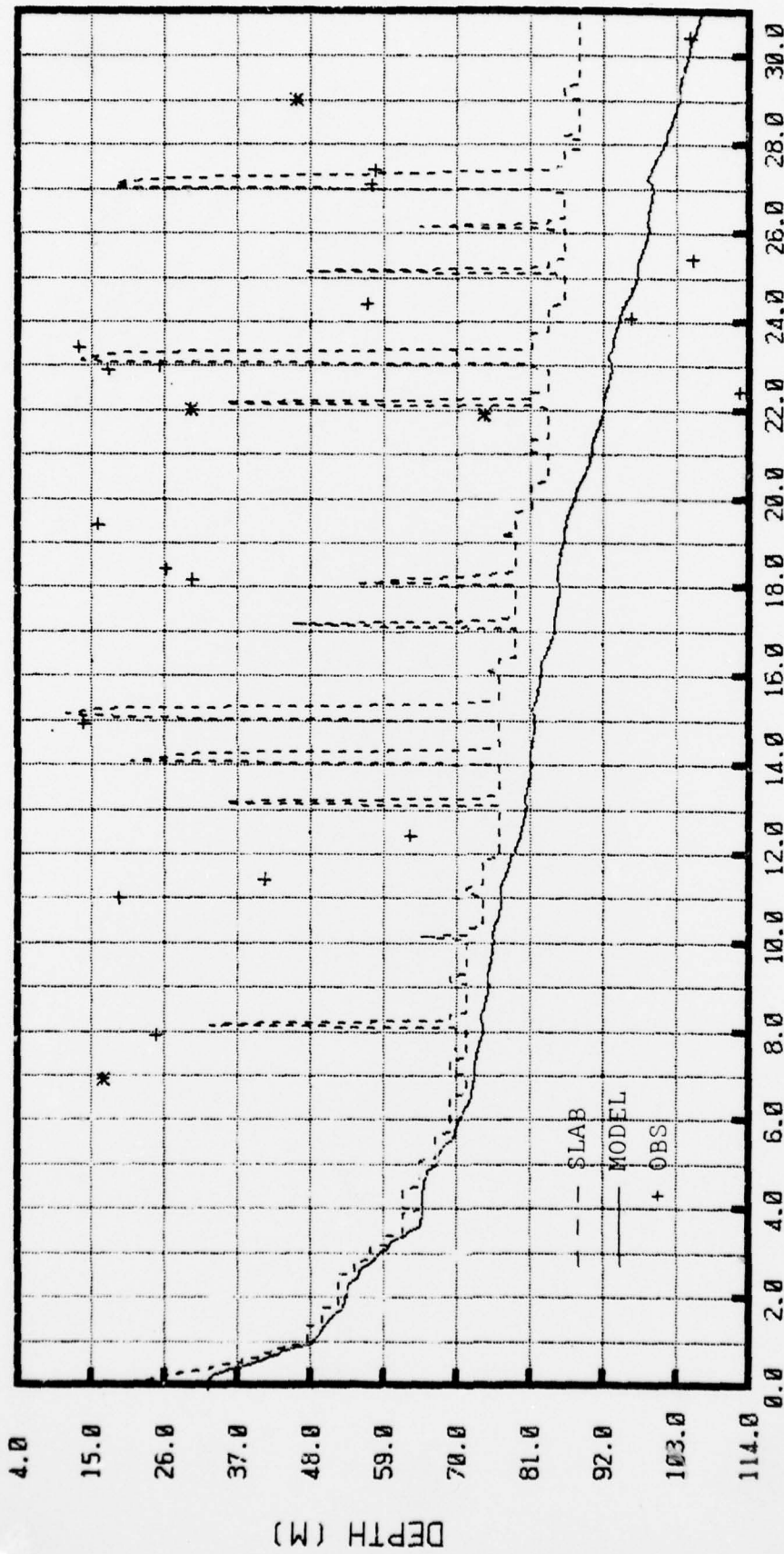
DAYS FROM 2814Z NOV 74

Figure 24. Surface salinity at OS HOTEL - 14 GMT 28 November to 14 GMT 29 December 1974, neglecting (E-P) and using a typical salinity profile.



DAYS FROM 2814Z NOV 74

Figure 25. Mixed-layer temperature at OS HOTEL - 14 GMT 28 November to 14 GMT 29 December 1974 from typical profile initialization.



DAYS FROM 2814Z NOV 74

Figure 26. Mixed-layer depth at OS HOTEL - 14 GMT 28 November to 14 GMT 29 December 1974 from typical profile initialization.

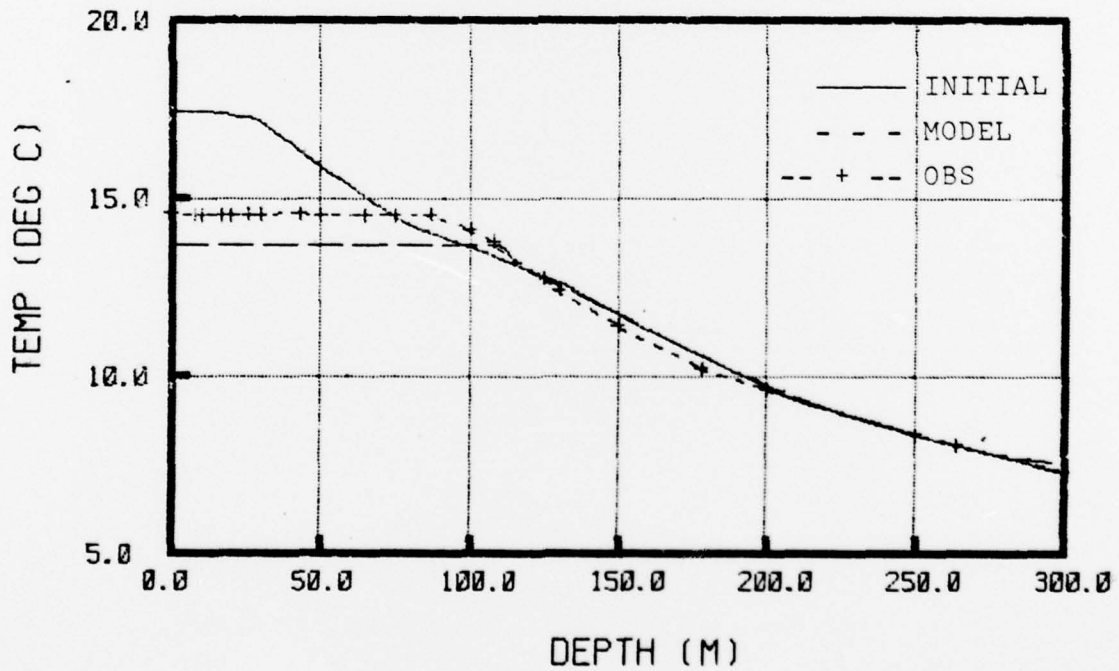
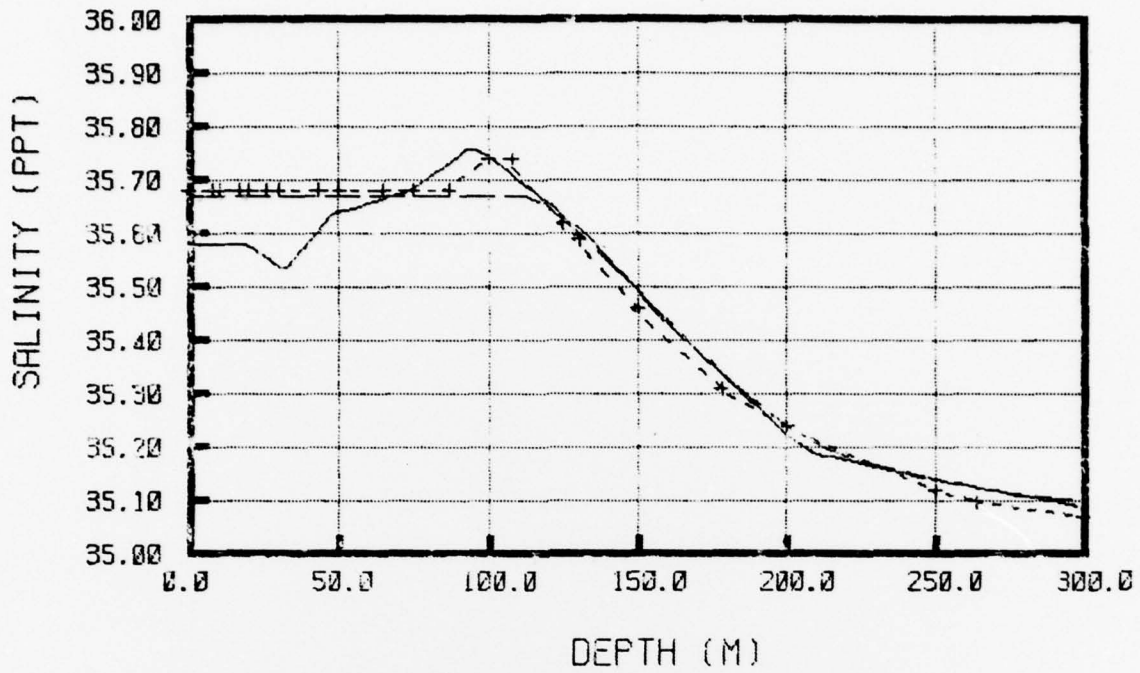
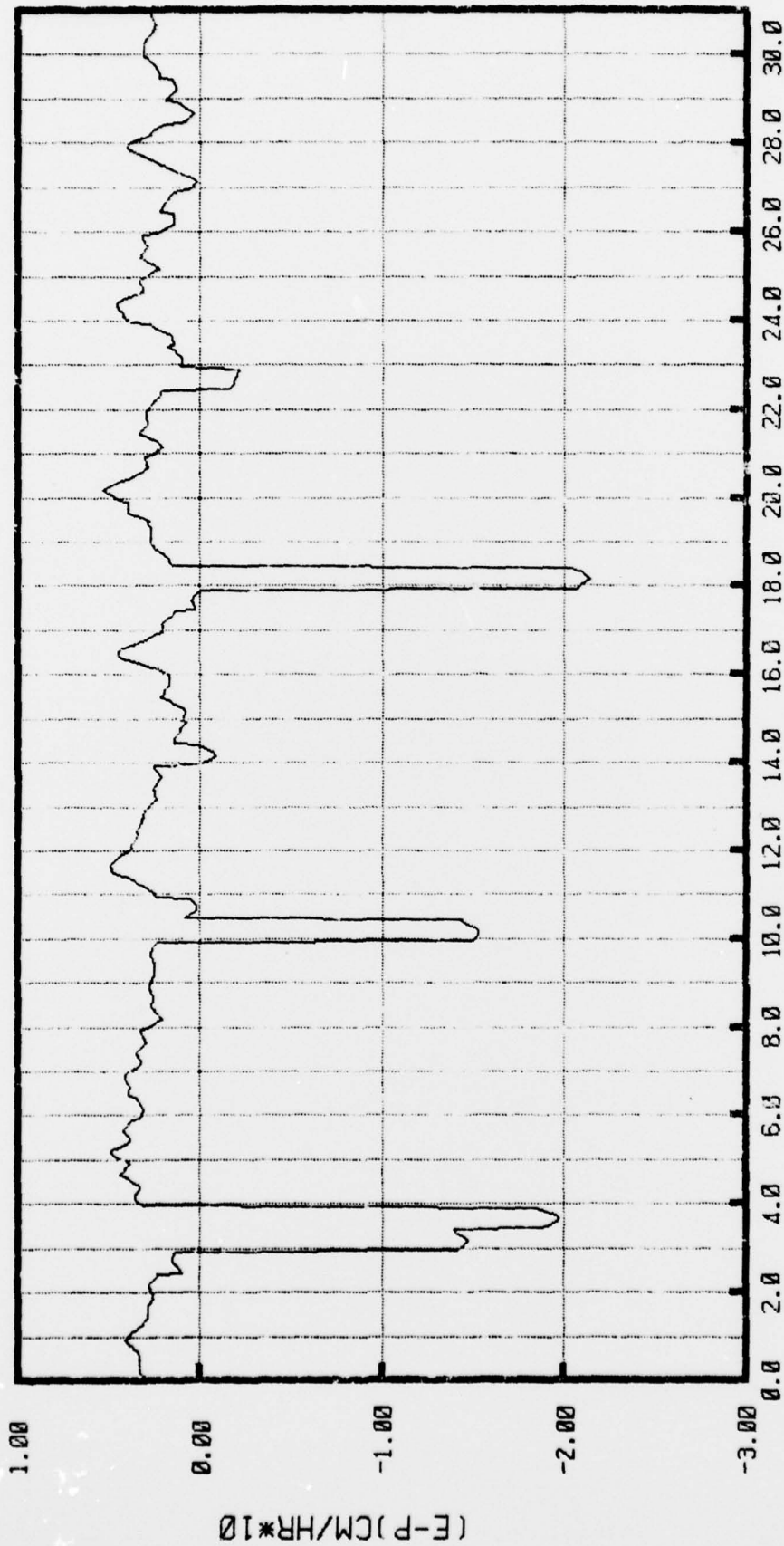
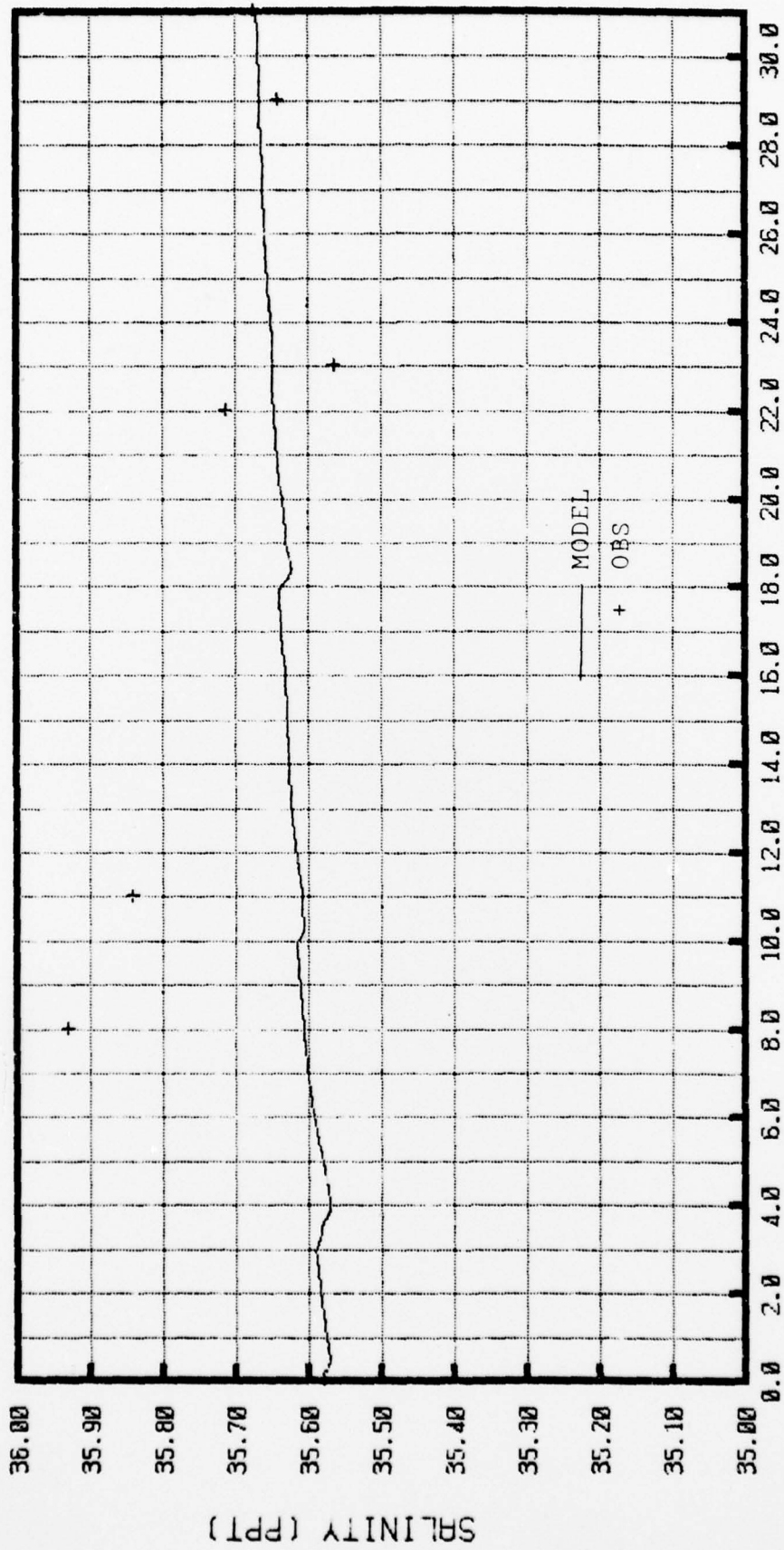


Figure 27. Depth vs temperature and salinity at OS HOTEL - 14 GMT 28 November and 14 GMT 29 December 1974, hydrocast data.



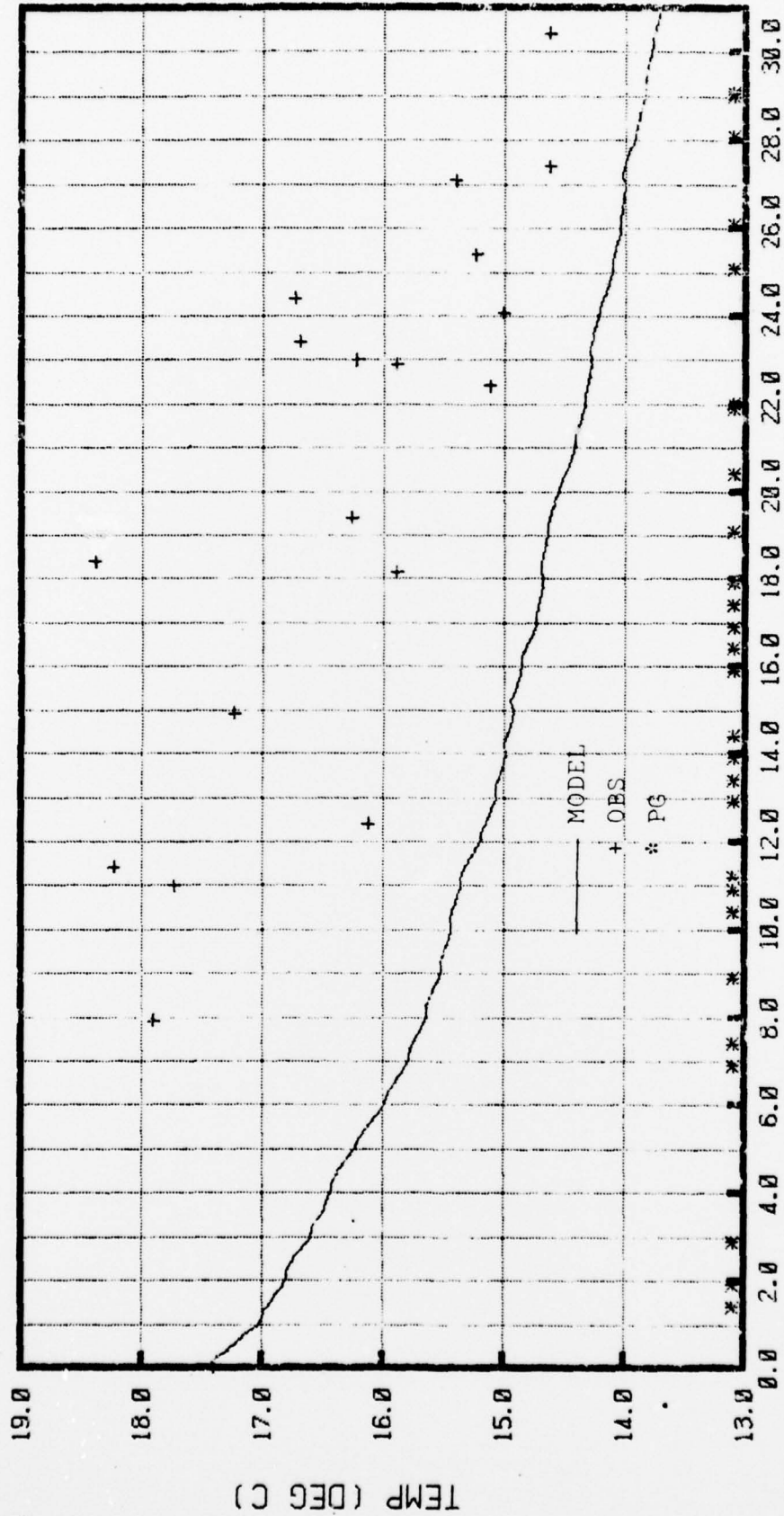
DAYS FROM 2814Z NOV 74

Figure 28. (E-P) at OS HOTEL - 14 GMT 28 November to 14 GMT 29 December 1974.



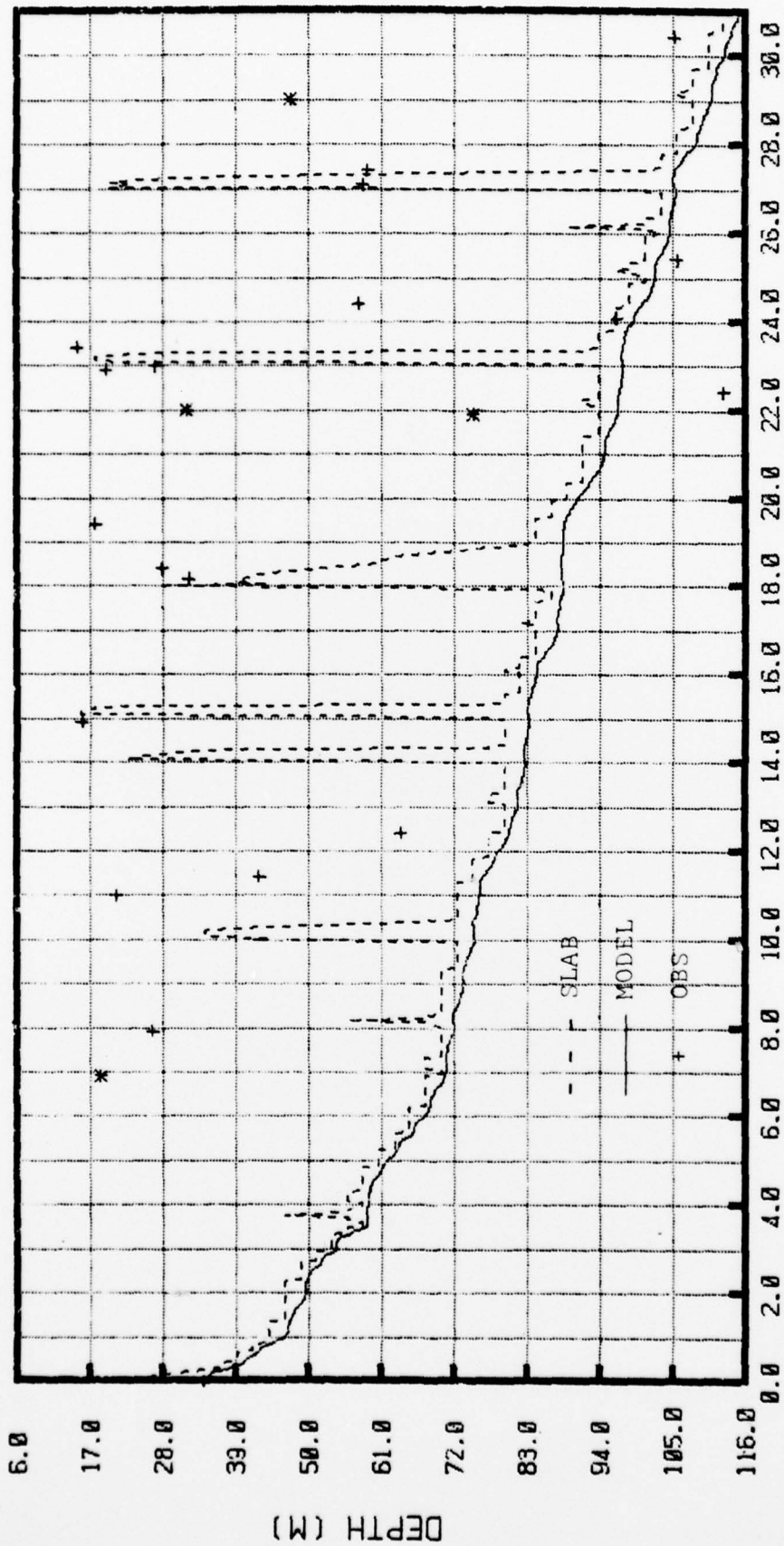
DAYS FROM 2814Z NOV 74

Figure 29. Surface salinity at OS HOTEL - 14 GMT 28 November to 14 GMT 29 December 1974.



DAYS FROM 2814Z NOV 74

Figure 30. Mixed-layer temperature at OS HOTEL - 14 GMT 28 November to 14 GMT 29 December 1974.



DAYS FROM 2814Z NOV 74

Figure 31. Mixed-layer depth at OS HOTEL - 14 GMT 28 November to 14 GMT 29 December 1974.

## LIST OF REFERENCES

- Camp, N. T., 1976: Role of strong atmospheric forcing events in the modification of the upper thermal structure during the cooling season. Ph.D. thesis, Naval Postgraduate School, 175 pp.
- Camp, N.T. and R. L. Elsberry, 1978: Ocean thermal response to strong atmospheric forcing. II. The role of one dimensional processes. J. Phys. Oceanogr., To appear in a forthcoming issue.
- Elsberry, R. L., T. S. Fraim, R. N. Trapnell, 1976: A mixed-layer model of the oceanic thermal response to hurricanes. J. Geophys. Res., 81, 1153-1162.
- Elsberry, R. L. and N.T. Camp, 1978: Ocean thermal response to strong atmospheric forcing. I. Characteristics of forcing events. J. Phys. Oceanogr., To appear in a forthcoming issue.
- Garwood, R. W., Jr., 1977: An oceanic mixed-layer model capable of simulating cyclical states. J. Phys. Oceanogr., 7, 455-468.
- Haney, R. L. and R. W. Davis, 1976: The role of surface mixing in the seasonal variation of the ocean thermal structure. J. Phys. Oceanogr., 6, 504-510.
- Institute of Ocean Sciences, 1975: Oceanographic Observations at Ocean Station P. Unpublished manuscript.
- Johnson, W. F., 1977: Upper ocean thermal structure forecast evaluation of a model using synoptic data. M.S. thesis, Naval Postgraduate School, 47 pp.
- Kraus, E. B. and J. S. Turner, 1967: A one-dimensional model of the seasonal thermocline. II. The general theory and its consequences. Tellus, 19, 98-106.
- Miller, J. R., 1976: The salinity effect in a mixed layer ocean model. J. Phys. Oceanogr., 6, 29-35.
- Ocean Data Systems, Inc., 1977: Hydroclimatological Data Retrieval Program. Unpublished manuscript.
- Thompson, R.O.R.Y., 1976: Climatological numerical models of the surface mixed layers of the ocean. J. Phys. Oceanogr., 6, 496-503.

INITIAL DISTRIBUTION LIST

	No. Copies
1. Defense Documentation Center Cameron Station Alexandria, Virginia 22314	2
2. Library, Code 0142 Naval Postgraduate School Monterey, California 93940	2
3. Director Naval Oceanography and Meteorology National Space Technology Laboratories Bay St. Louis, Mississippi 39520	1
4. Professor R. L. Elsberry, Code 63Es Department of Meteorology Naval Postgraduate School Monterey, California 93940	8
5. Professor G. J. Haltiner, Code 63Ha Chairman, Department of Meteorology Naval Postgraduate School Monterey, California 93940	1
6. Department of Oceanography, Code 68 Naval Postgraduate School Monterey, California 93940	1
7. Lieutenant R. A. Paulus Naval Ocean System Center, Code 035 271 Catalina Blvd. San Diego, California 92152	2
8. Commanding Officer Fleet Numerical Weather Central Monterey, California 93940	2
9. Naval Oceanographic Research and Development Agency, Code 0201 Bay St. Louis, Mississippi 39520	1
10. Professor R. L. Haney, Code 63Hy Department of Meteorology Naval Postgraduate School Monterey, California 93940	1
11. Professor R. W. Garwood, Code 68Gd Department of Oceanography Naval Postgraduate School Monterey, California 93940	1

- |     |  |   |
|-----|--|---|
| 12. | Lieutenant V. F. Looft<br>Naval Weather Service<br>Environmental Detachment<br>Moffett Field, California 94035 | 1 |
| 13. | Lieutenant S. M. Schrobo<br>OA Division<br>USS KITTY HAWK (CV-63)<br>FPO San Francisco 96601                   | 1 |
| 14. | Lieutenant M. G. Salinas<br>Naval Support Forces Antarctica<br>Met. Div., Code 030<br>FPO San Francisco 96601  | 1 |